Taylor & Francis
Taylor & Francis Group

Quality Engineering

ISSN: (Print) (Online) Journal homepage: https://www.tandfonline.com/loi/lqen20

Simultaneous monitoring of the mean vector and covariance matrix of multivariate multiple linear profiles with a new adaptive Shewhart-type control chart

Hamed Sabahno & Amirhossein Amiri

To cite this article: Hamed Sabahno & Amirhossein Amiri (2023) Simultaneous monitoring of the mean vector and covariance matrix of multivariate multiple linear profiles with a new adaptive Shewhart-type control chart, Quality Engineering, 35:4, 600-618, DOI: 10.1080/08982112.2022.2164725

To link to this article: https://doi.org/10.1080/08982112.2022.2164725

© 2023 The Author(s). Published with license by Taylor & Francis Group, LLC.

Published online: 13 Jan 2023.

Submit your article to this journal

Article views: 996

View related articles

View Crossmark data

Citing articles: 2 View citing articles

Full Terms & Conditions of access and use can be found at
https://www.tandfonline.com/action/journalInformation?journalCode=lqen20

QUALITY ENGINEERING
2023, VOL. 35, NO. 4, 600–618
https://doi.org/10.1080/08982112.2022.2164725

Taylor & Francis
Taylor & Francis Group

OPEN ACCESS Check for updates

Simultaneous monitoring of the mean vector and covariance matrix of multivariate multiple linear profiles with a new adaptive Shewhart-type control chart

Hamed Sabahno[a] and Amirhossein Amiri[b]

[a]Department of Statistics, School of Business, Economics and Statistics, Umeå University, Umeå, Sweden; [b]Department of Industrial Engineering, Faculty of Engineering, Shahed University, Tehran, Iran

ABSTRACT
There has been a growing interest in research regarding monitoring a process through a regression model (called a profile) rather than a simple quality characteristic. This paper proposes a new monitoring scheme to simultaneously monitor the multivariate multiple linear profiles' parameters. This scheme is based on the Shewhart control chart concept and only has one single (max-type) control chart for monitoring regression coefficients and error's variation, which uses a new statistic to improve the variability (error's variance-covariance matrix) shift detection in multivariate profiles. To increase the sensitivity and capability of the proposed scheme, especially in detecting small to moderate shift sizes, we add a variable parameters (VP) adaptive scheme to the developed control chart as well, considering that no adaptive monitoring schemes have so far been developed for monitoring the multivariate multiple linear profiles and neither are there any VP adaptive features for all profile monitoring schemes. Next, we develop a Markov chain model to compute the time to signal and run length performance measures. After that, we perform extensive numerical analyses to first compare the proposed control chart with the best available control charts and then evaluate its performance under different shift scenarios as well as different dimensions. The results show that the new monitoring scheme performs well compared to the best available monitoring schemes, and more importantly, it is more applicable in real practice. Finally, an illustrative example is presented to show the implementation of the proposed scheme in practice.

KEYWORDS
adaptive control charts; Markov chains; max-type control charts; multivariate analysis; multivariate multiple linear profiles; profile monitoring

1. Introduction

In some cases, instead of a single measurement of quality characteristics, a relationship between one response variable and one or more explanatory variables characterizes the quality of the process or product. This functional relationship, which is in the form of a regression model, is called a profile. The procedure of investigating whether this regression model remains statistically the same throughout time is called "profile monitoring" in the statistical process monitoring literature. If the linear regression model has more than one explanatory variable, it is called a multiple linear profile; otherwise, it is called a simple linear profile. In addition, if there are multiple response variables that are correlated to one another, multivariate profile monitoring schemes should be used. Profiles come in different shapes and forms. However, the focus of this paper is only on linear profiles (linear regression models). Due to the nature of linear profiles, most researchers who work in this area assume that the explanatory variables only vary within samples and not between samples. That is one of the assumptions of this paper as well. In addition, another focus of this paper is on Phase II schemes in which the profile parameters (intercept, slopes, and error's variance-covariance matrix) are assumed known prior to the online process monitoring (for an example of non-linear profiles in both Phase-I, with estimated parameters, and Phase-II, with known parameter values, see Fan, Jen, and Lee 2017).

Simple linear profiles were introduced by Kang and Albin (2000) with two applications: one in semiconductor manufacturing and the other in food

CONTACT Hamed Sabahno hamed.sabahno@umu.se Department of Statistics, School of Business, Economics and Statistics, Umeå University, Umeå 901 87, Sweden.

© 2023 The Author(s). Published with license by Taylor & Francis Group, LLC.
This is an Open Access article distributed under the terms of the Creative Commons Attribution-NonCommercial-NoDerivatives License (http://creativecommons.org/licenses/by-nc-nd/4.0/), which permits non-commercial re-use, distribution, and reproduction in any medium, provided the original work is properly cited, and is not altered, transformed, or built upon in any way.

manufacturing, where an artificial sweetener was characterized by a profile. They proposed two control charts: one based on Hotelling's T^2 approach and the other based on a memory-type EWMA (exponentially weighted moving average) approach. Another major improvement in profile monitoring was made by Kim, Mahmoud, and Woodall (2003) who proposed three exponentially weighted moving average (called EWMA-3) control charts to monitor simple linear profile's parameters.

In the case of multivariate profiles, another focus of this paper, Noorossana, Eyvazian, and Vaghefi (2010a), employed three control charts based on a MEWMA (Multivariate EWMA) control chart to monitor the multivariate simple linear profiles. Eyvazian et al. (2011) employed four approaches for monitoring the multivariate multiple linear regression profiles (MMLRPs) in the case of known parameters. Zou, Ning, and Tsung (2012) developed a LASSO-based multivariate profile to overcome the problem of large dimensionality as well as to identify the shifted variables. Soleimani, Noorossana, and Niaki (2013) investigated the autocorrelation within profiles in multivariate simple linear profiles, and Amiri et al. (2014) proposed some methods for monitoring the MMLRPs to identify which profiles or parameters have shifted after the chart's signal. In addition, Soleimani and Noorossana (2014) investigated the autocorrelation between profiles in multivariate simple linear profiles, and Ayoubi, Kazemzadeh, and Noorossana (2014) developed a maximum likelihood estimator to estimate the change point when a monotonic shift occurs in the mean of response variables in multivariate linear profiles.

One of the most common applications of multivariate linear profiles has so far been in the calibration of measurement systems, such as the relationship between the nominal and real forces in car cylinders (Noorossana, Eyvazian, and Vaghefi 2010a), force balance calibration in an aircraft (Eyvazian et al. 2011), and the calibration case of an electrical torquemeter measuring the torque required to fasten twins in a car (Ayoubi, Kazemzadeh, and Noorossana 2014). However, there are some other applications reported as well. For example, Zou, Ning, and Tsung (2012) used multivariate multiple linear profiles in a logistic company (a loading process) for a different type of calibration, with the response variables being the daily job frequency and the daily average time to complete the job (both response variables together show the efficiency and the capability of the process), with five explanatory variables to predict the response values. Also, Soleimani, Noorossana, and Niaki (2013) used multivariate profiles in a machining process, where the response variables were the cost of machining and the tool's life, and with the cutting speed as the explanatory variable. For more information about different types of profile monitoring schemes, we refer the interested readers to Maleki, Amiri, and Castagliola (2018) who performed a literature review on this subject.

Simultaneous monitoring of the process parameters (the mean vector and variance-covariance matrix) is usually preferred over monitoring only one of them, due to its better overall performance. There are two main simultaneous monitoring schemes: i) single-chart schemes (one statistic/control limit/chart for both process parameters) and ii) double-chart schemes (one statistic/control limit/chart for each process parameter). However, using a single-chart scheme is usually preferred in practice due to its simplicity of usage. Several simultaneous monitoring schemes have been proposed for multivariate processes. Among which are the following: Khoo (2004), Chen, Cheng, and Xie (2005), Zhang, Li, and Wang (2010), Wang, Yeh, and Li (2014), Sabahno, Castagliola, and Amiri (2020a, 2020b), and Sabahno, Amiri, and Castagliola (2021).

Some research is also available for simultaneous monitoring of the profiles' parameters. Zhang, Li, and Wang (2009) proposed the ELR control chart for simultaneously monitoring the mean and variance in simple linear profiles. Eyvazian et al. (2011) extended the ELR control chart developed by Zhang, Li, and Wang (2009) for monitoring the multivariate multiple linear regression profiles and called it the ELRT control chart. Khedmati and Niaki (2016) proposed a Max-EWMA3 control chart based on the adjusted parameter estimates for simultaneous monitoring of the parameters of a simple linear profile in multistage processes. Moreover, Ghashghaei and Amiri (2017a) proposed Max-MEWMA and Max-MCUSUM (multivariate cumulative sum) control charts for simultaneous monitoring of the mean vector and variance-covariance matrix of the MMLRPs. Ghashghaei and Amiri (2017b) also developed the sum of squares control charts: SS- MEWMA and SS-MCUSUM for Phase II monitoring of the MMLRPs. Ghashghaei, Amiri, and Khosravi (2019) furthermore developed SC-MGWMA (semi-circle-multivariate general weighted moving average) and SC-MEWMA control charts for monitoring the MMLRPs. Finally, Malela-Majika, Chatterjee, and Koukouvinos (2022) investigated and compared different max-type univariate and multivariate control charts based on single, double, and triple EWMA statistics, including in the cases of fixed and random explanatory variables. They computed the performance measures using the Monte Carlo simulation method.

To the best of our knowledge, the simultaneous monitoring schemes developed for profile monitoring are all based on memory-type control charts (based on either EWMA/GWMA or CUSUM statistics).

The Shewhart control chart was introduced in 1924 and with it the concept of statistical process monitoring started developing. Since then, many other control charts have been developed; nevertheless, since Shewhart-type control charts are designed regardless of the shift size (which is usually unknown in real practice), none are as practical as Shewhart-type control charts in the real world. Shewhart-type control charts are memoryless control charts and that is why they are slow in detecting small to moderate shifts from baselines/targets. To overcome this problem, memory-type control charts such as EWMA and CUSUM charts were developed. However, the main drawback of using these types of control charts is that one should know what shift size is expected from the process and tune the control chart and determine its main parameter, which in the case of the EWMA chart is the smoothing parameter and in case of the CUSUM chart the reference value, accordingly. This is not, however, the case in most practical applications, considering that the expected shift size is usually unknown. This makes it more practical to improve the Shewhart-type control charts and increase their sensitivity instead of using memory-type control charts. Classical Shewhart control charts have fixed parameters (FP). To increase their sensitivity in detecting small to moderate shift sizes, adaptive control charts were developed. Adaptive control charts are dynamic methods that use previous process sampling information to determine the chart parameters' values for the next sampling. In adaptive control charts, at least one of the chart's parameters, namely sample size, sampling interval, and control limits, are allowed to vary throughout the online process monitoring. If all three parameters are allowed to vary, then the scheme is called a variable parameters (VP) scheme. Research such as that by Sabahno, Amiri, and Castagliola (2021) have shown that using VP control charts is the best adaptive approach in terms of performance. However, there is a drawback in using adaptive control charts as well. That is the added complexity in administrating the adaptive control charts. Research has also shown that having only two types of chart parameters is the best approach to have both performance improvement and administrative simplicity (Jensen, Bryce, and Reynolds 2008).

Adding adaptive features in profile monitoring schemes has rarely been investigated. The available studies are the following. Zhang, Li, and Wang (2009), along with proposing the ELR chart, added a variable sampling intervals (VSI) adaptive feature to improve its performance, and Li and Wang (2010) added a VSI adaptive feature to the EWMA-3 chart. Abdella, Yang, and Alaeddini (2014) added a variable sample size and sampling interval (VSSI) adaptive feature to the Hotelling's T^2 chart and investigated its optimal design. Furthermore, Ershadi, Noorossana, and Niaki (2016a) investigated the statistical-economic design of a VSI EWMA chart, whereas Magalhaes and Von Doellinger (2016) added a variable sample size (VSS) adaptive feature to the Hotelling's T^2 chart for monitoring the simple linear profiles and evaluated its performance using a Markov chain model. In a further study, Kazemzadeh, Amiri, and Kouhestani (2016) added a VSS feature to both EWMA-3 and MEWMA control charts, and Ershadi, Noorossana, and Niaki (2016b) did the same as Ershadi, Noorossana, and Niaki (2016a), but this time they investigated the economic design of a VSS T^2 chart. Hafez Darbani and Shadman (2018) combined the concepts of generalized likelihood ratio and variable sampling interval. Finally, Yeganeh, Abbasi, and Shongwe (2021) developed a new adaptive scheme based on a varying memory-type statistic for monitoring multiple linear profiles and evaluated the chart's performance using simulation runs. To the best of our knowledge, no VP adaptive charts have been developed so far in the profile monitoring literature. In addition, no adaptive feature has so far been added to the multivariate multiple linear profiles.

In this paper, we propose a Shewhart-type scheme for simultaneously monitoring the MMLRPs' parameters with a single control chart. We develop a new scheme in which we also propose a new statistic to enhance the control chart's performance in detecting the multivariate profiles' variability. To improve the performance of the control chart and make it comparable to the best available MMLRP monitoring methods, we add adaptive features to the proposed scheme, which have not been considered before concerning any MMLRPs control schemes. We also, for the first time in the profile monitoring field, consider VP adaptive schemes. In addition, we develop a Markov chain model and use it to compute the time to signal and run length performance measures, by which we compare the proposed scheme to some of the best performing available control charts, namely ELRT, Max-MEWMA, and Max-MCUSUM.

In the next section of this paper, the multivariate multiple linear profiles (MMLRPs) are explained. In Section 3, the proposed control chart is developed. The VP adaptive feature will be added to the proposed control chart in Section 4. Markov chains-based performance measures are developed in Section 5, and numerical analyses, which include comparisons with other charts as well as extensive evaluations under different shift scenarios and different dimensions, are performed in Section 6. In Section 7, an illustrative example is presented based on a real industrial case. Finally, conclusions and suggestions for future developments are mentioned in Section 8.

2. Multivariate multiple linear profiles

For the kth sample of size n, with p response variables, $\mathbf{Y}_k$ is a $n \times p$ matrix. $\mathbf{Y}_k$ is a linear function of some independent variables x, so that:

$$\mathbf{Y}_k = \mathbf{X}\mathbf{B} + \mathbf{E}_k, \tag{1}$$

where $\mathbf{X}$ is a $n \times (q+1)$ matrix of explanatory (independent) variables, q is the number of independent variables, $\mathbf{B}$ is a $(q+1) \times p$ matrix of regression parameters, and $\mathbf{E}_k$ is a $n \times p$ matrix of correlated error terms (ε), which follows a multivariate normal distribution $(\mathbf{0}, \boldsymbol{\Sigma})$, where $\boldsymbol{\Sigma} = \begin{pmatrix} \sigma_{11} & \sigma_{12} & \cdots & \sigma_{1p} \\ \vdots & & \ddots & \vdots \\ \sigma_{p1} & \sigma_{p2} & \cdots & \sigma_{pp} \end{pmatrix}$, and σ_{gh} denotes the covariance between the error vector terms of gth and hth response variables at each observation.

Therefore, we can write Equation (1) as:

$$\begin{pmatrix} y_{11k} & y_{12k} & \cdots & y_{1pk} \\ \vdots & & \ddots & \vdots \\ y_{n1k} & y_{n2k} & \cdots & y_{npk} \end{pmatrix} = \begin{pmatrix} 1 & x_{11} & \cdots & x_{1q} \\ \vdots & & \ddots & \vdots \\ 1 & x_{n1} & \cdots & x_{nq} \end{pmatrix}_{n\times(q+1)} \begin{pmatrix} \beta_{01} & \beta_{02} & \cdots & \beta_{0p} \\ \vdots & & \ddots & \vdots \\ \beta_{q1} & \beta_{q2} & \cdots & \beta_{qp} \end{pmatrix}_{(q+1)\times p} + \begin{pmatrix} \varepsilon_{11k} & \varepsilon_{12k} & \cdots & \varepsilon_{1pk} \\ \vdots & & \ddots & \vdots \\ \varepsilon_{n1k} & \varepsilon_{n2k} & \cdots & \varepsilon_{npk} \end{pmatrix}_{n\times p}.$$

The above model is called a multivariate $(p > 1)$ multiple $(q > 1)$ linear profile. If $p=1$ and/or $q=1$, the linear profile cannot be called a multivariate and/or a multiple model. In the case of $p=q=1$, the model is called a simple linear profile.

3. A max-type control chart

In this section, we develop a single control chart for simultaneously monitoring the process mean and variability ($\mathbf{B}$ and $\boldsymbol{\Sigma}$ matrices), in which their values are assumed known.

First, we develop a statistic to represent the process mean vector. To monitor the process mean, we use the Hotelling's T_k^2 statistic to monitor the changes in $\mathbf{B}$. The sample estimate of the $\mathbf{B}$ matrix $(\hat{\mathrm{B}}_k)$ is computed as:

$$\hat{\mathrm{B}}_k = [\mathbf{X}^T\mathbf{X}]^{-1}\mathbf{X}^T\mathbf{Y}_k.$$

By changing $\hat{\mathrm{B}}_k$ into a $p(q+1) \times 1$ vector, we have:

$$\hat{\boldsymbol{\beta}}_k = \left(\hat{\beta}_{01k}, \hat{\beta}_{11k}, \ldots, \hat{\beta}_{q1k}, \ldots\ldots, \hat{\beta}_{0pk}, \hat{\beta}_{1pk}, \ldots, \hat{\beta}_{qpk}\right)^T. \tag{2}$$

Next, we need to compute its average and variance-covariance matrix. For an in-control process, and since we assume that the parameters' values are known, the expected value of $\hat{\mathrm{B}}_k$ is equal to $\mathbf{B}$. Therefore, we have:

$$\boldsymbol{\beta} = \mathrm{E}(\hat{\boldsymbol{\beta}}_k) = \left(\beta_{01}, \beta_{11}, \ldots, \beta_{q1}, \ldots\ldots, \beta_{0p}, \beta_{1p}, \ldots, \beta_{qp}\right)^T. \tag{3}$$

For its variance-covariance matrix, we have:

$$\boldsymbol{\Sigma}_{\hat{\boldsymbol{\beta}}_k} = \begin{pmatrix} \boldsymbol{\Sigma}_{11} & \boldsymbol{\Sigma}_{12} & \cdots & \boldsymbol{\Sigma}_{1p} \\ \vdots & & \ddots & \vdots \\ \boldsymbol{\Sigma}_{p1} & \boldsymbol{\Sigma}_{p2} & \cdots & \boldsymbol{\Sigma}_{pp} \end{pmatrix}_{p(q+1)\times p(q+1)}, \tag{4}$$

whereas detailed in Eyvazian et al. (2011), $\boldsymbol{\Sigma}_{gh}$ is a $(q+1) \times (q+1)$ matrix equal to $[\mathbf{X}^T\mathbf{X}]^{-1}\sigma_{gh}$.

Subsequently, by using Equations (2)–(4), the Hotelling's T^2 statistic for sample k is computed as:

$$T_k^2 = \left(\hat{\boldsymbol{\beta}}_k - \boldsymbol{\beta}\right)^T \boldsymbol{\Sigma}_{\hat{\boldsymbol{\beta}}_k}^{-1}\left(\hat{\boldsymbol{\beta}}_k - \boldsymbol{\beta}\right), \tag{5}$$

which when the process is in-control, follows a chi-square distribution with $p(q+1)$ degrees of freedom.

Second, to monitor the process variability, we first define the sum of the squared residuals (**SSE**) of sample k, as:

$$\begin{aligned} \mathbf{SSE}_k &= (\mathbf{Y}_k - \mathbf{X}\hat{\mathrm{B}}_k)^T(\mathbf{Y}_k - \mathbf{X}\hat{\mathrm{B}}_k) = \mathbf{Y}_k'\mathbf{Y}_k - \hat{\mathbf{B}}_k'\mathbf{X}'\mathbf{Y}_k \\ &= \mathbf{E}_k^T\mathbf{E}_k. \end{aligned} \tag{6}$$

where $\mathbf{SSE}_k$ follows a p-variate Wishart distribution $(\boldsymbol{\Sigma}, n)$. Then, for the mean of squared residuals (**MSE**) of sample k, when the process is in-control, we have:

$$\mathbf{MSE}_k = \frac{\mathbf{SSE}_k}{n} \sim \frac{1}{n} W_p(\boldsymbol{\Sigma}, n). \tag{7}$$

$\mathbf{MSE}_k$ is an unbiased estimator of the variance-covariance matrix of errors ($\boldsymbol{\Sigma}$).

Note that, in the case of unknown values for the model parameters ($\mathbf{B}$ and $\boldsymbol{\Sigma}$), one can easily estimate them by performing a Phase I analysis. This is done by taking m profiles ($k = 1, \ldots, m$) from the process, estimating the parameters' values for each profile, omitting the out-of-control profiles, and finally taking their average values under an in-control state. More precisely, to estimate $\boldsymbol{\beta}$, we compute $\hat{\boldsymbol{\beta}}_k$ for each profile using Equation (2), and then we take the average of all the $\hat{\boldsymbol{\beta}}_k$ values under an in-control state. Similarly, $\boldsymbol{\Sigma}$ is estimated by computing $\mathbf{MSE}_k$ for each profile using Equation (7), again taking the average values of m profiles when the process is stable. For more details on and methods for estimating the multivariate multiple linear regression profiles' parameters in Phase I, we refer interested readers to Noorossana et al. (2010b). Moreover, when estimating the process parameters, the more the number of samples (m) in Phase I, the better the parameters estimation. The minimum number of samples should be determined so that the desired performance of the control chart in Phase II in terms of the in-control ARL (average run length) is achieved. If the minimum value of m to achieve the desired in-control ARL in Phase II is too large, which might not be feasible in practice, another method is to adjust the control limits with any feasible value of m to obtain the desired performance. For more information regarding the effect of parameters estimation in Phase I on the control charts' performance in Phase II, we refer interested readers to Jensen et al. (2006).

To be able to develop a control chart for monitoring $\mathbf{MSE}$, we need to change it into a number.

Let us first assume any fixed $p \times 1$ vector $\mathbf{a}$; then by definition we have:

$$\mathbf{a}^T\mathbf{SSE}\ \mathbf{a}\ \sim (\mathbf{a}^T\boldsymbol{\Sigma}\ \mathbf{a})\ \chi^2_n, \tag{8}$$

where $\frac{\mathbf{a}^T\mathbf{SSE}\ \mathbf{a}}{\mathbf{a}^T\boldsymbol{\Sigma}\ \mathbf{a}}$ is independent of $\mathbf{a}$.

Consequently, by replacing $\mathbf{SSE}$ with $\mathbf{MSE}$, we have:

$$V_k = \mathbf{a}^T\mathbf{MSE}_k\ \mathbf{a}\ \sim \frac{\mathrm{a}^T\Sigma\ \mathrm{a}}{n}\chi^2_n. \tag{9}$$

Note that, if $\mathbf{a}$ is chosen to be a vector of 1 s, then $\mathbf{a}^T\mathbf{MSE}\ \mathbf{a}$ is the summation of all the elements of the variance-covariance matrix $\mathbf{MSE}$. Therefore, we choose $\mathbf{1}$ as the default value for $\mathbf{a}$. In addition, if $\mathbf{a}$ is a positive vector of 2 s or 3 s, $\ldots$, then $\mathbf{a}^T\mathbf{MSE}\ \mathbf{a}$ is the summation of all the elements of $\mathbf{MSE}$ multiplied by 2^2 or $3^2, \ldots$. Moreover, as long as vector $\mathbf{a}$ has equal elements, the after-mentioned chart's performance would not change if the value of $\mathbf{a}$ changes; i.e., the control chart's performance would be insensitive to the value of $\mathbf{a}$.

Finally, if we define: $b = \frac{\mathbf{a}^T\boldsymbol{\Sigma}\ \mathbf{a}}{n}$, then by definition, if $b > 0$, V_k follows a gamma distribution as:

$$V_k\ \sim Gamma\left(\frac{n}{2}, 2b\right). \tag{10}$$

Note that, since the value of vector $\mathbf{a}$ is arbitrary, in the case where the default value of $\mathbf{a} = \mathbf{1}$ does not satisfy $b > 0$, we can choose any other value for $\mathbf{a}$, provided that it satisfies the condition. However, for $\mathbf{a} = \mathbf{1}$ not to be able to satisfy $b > 0$, covariances should be negative and very large, which is very unlikely.

To simultaneously monitor the mean (regression coefficients) and variability (errors' variance-covariance matrix) of the multivariate multiple linear profiles, we first normally standardize the T^2_k and V_k statistics, respectively, as:

$$ST^2_k = \Phi^{-1}\left[F_{p(q+1)}\left(T^2_k\right)\right], \tag{11}$$

$$SV_k = \Phi^{-1}\left[\Gamma_{\frac{n}{2}, 2b}\left(V^2_k\right)\right], \tag{12}$$

where $\Phi(.)$ is the standard normal cumulative distribution function, $F_{p(q+1)}(.)$ denotes the chi-square cumulative distribution function with $p(q+1)$ degrees of freedom and $\Gamma_{\frac{n}{2}, 2b}(.)$ represents the gamma cumulative distribution function with the shape parameter $\frac{n}{2}$ and the scale parameter $2b$. Both ST^2_k and SV_k independently follow a standard normal distribution (0,1).

Then, we use a single statistic to represent both statistics as:

$$SS_k = \max\left\{|ST^2_k|, |SV_k|\right\}. \tag{13}$$

Since the larger absolute values between ST^2_k and SV_k are always considered when computing SS_k, we only need an upper control limit (UCL) for this control chart, and it is obtained by solving: $P(SS_k \le UCL) = 1 - \alpha$, where α is the probability of Type-I error. Then, we have:

$$\begin{aligned} P(SS_k \le UCL) &= P\left(\max\left\{|ST^2_k|, |SV_k|\right\} \le UCL\right) \\ &= P\left(|ST^2_k| \le UCL\right)P(|SV_k| \le UCL) \\ &= (2\Phi(UCL) - 1)^2. \end{aligned} \tag{14}$$

Consequently, after some simple algebraic computations, we have:

$$UCL = \Phi^{-1}\left(\frac{\sqrt{1-\alpha}+1}{2}\right). \tag{15}$$

4. A VP adaptive scheme

There are several adaptive control charts. The VP (variable parameters) adaptive control charts have been proven to be the most effective ones. In such adaptive schemes, all the design (chart) parameters are allowed to vary during the online sampling. It has also been proven that having more than two design parameters' states, considering all the important factors (such as administrative complexity, sampling costs, and performance), is the most efficient one. In this paper, we develop a VP scheme and as in most adaptive control charts developed so far, two states (s) for each design parameter are considered ($s \in [1, 2]$), i.e., n_1 and n_2 for the sample sizes, t_1 and t_2 for the sampling intervals and, α_1 and α_2 for the Type-I error probabilities, with $n_1 < n_2$, $t_2 < t_1$ and $\alpha_1 < \alpha_2$. Consequently, we have two upper control limits UCL_1 and UCL_2, with $UCL_2 < UCL_1$. We should also have two upper warning limits UWL_1 and UWL_2, with $UWL_1 < UCL_1$ and $UWL_2 < UCL_2$. Then, the strategy for choosing the next sample's design parameters in a VP scheme is as follows:

- When SS_k is in the safe zone (i.e., $SS_k \in \left[0, UWL_{(k)}\right]$), the design parameters for the next sample are n_1, t_1, UCL_1, UWL_1.
- When SS_k is in the warning zone (i.e., $SS_k \in (UWL_{(k)}, UCL_{(k)}]$), the design parameters for the next sample are n_2, t_2, UCL_2, UWL_2.
- When SS_k is out of the safe zone (i.e., $SS_k \in (UCL_{(k)}, \infty)$), the process is called out-of-control and corrective actions are necessary.

Note that $UCL_{(k)} \in \{UCL_1, UCL_2\}$ and $UWL_{(k)} \in \{UWL_1, UWL_2\}$ are the upper control and warning limits used for sample $k = 1,2, \ldots$.

The following three equations are the VP control chart's equalities that should always be satisfied (each relates to one design parameter):

$$E(n) = n_1 P_0 + n_2(1 - P_0), \tag{16}$$

$$E(t) = t_1 P_0 + t_2(1 - P_0), \tag{17}$$

$$E(\alpha) = \alpha_1 P_0 + \alpha_2(1 - P_0), \tag{18}$$

where $E(n)$ is the average sample size, $E(t)$ is the average sampling interval, $E(\alpha)$ is the average Type-I error probability and P_0 is the probability of being in the safe zone while the process is in-control, i.e.,:

$$\begin{aligned} P_0 &= \frac{P(SS_k \le UWL)}{P(SS_k \le UCL)} \\ &= \frac{P(\max\{|ST_k^2|, |SV_k|\} \le UWL)}{P(\max\{|ST_k^2|, |SV_k|\} \le UCL)} \\ &= \frac{[2\Phi(UWL) - 1]^2}{[2\Phi(UCL) - 1]^2}. \end{aligned} \tag{19}$$

Note that we have three Equations (16)–(18) but more than three unknown design parameters. Therefore, the values of some of these parameters should be fixed and the others can be obtained using these equations. Researchers and practitioners usually fix the values of the sample sizes n_1 and n_2 (because above all, the system conditions and restrictions should determine their values), the smallest sampling interval t_2 (because being smaller than a certain value may not be possible for the quality system to handle) and the smallest Type-I error α_1 (management should determine what is "the lowest possible Type-I error probability"/"the largest possible UCL value" in the system). In addition, their average values ($E(n)$, $E(t)$, and $E(\alpha)$) are fixed as well (because they show what are the expected values of the chart parameters).

By solving Equations (16) and (17) together, t_1 and α_2 are obtained as:

$$t_1 = \frac{E(t)(n_1 - n_2) - t_2(n_1 - E(n))}{E(n) - n_2}, \tag{20}$$

$$\alpha_2 = \frac{E(\alpha)(n_1 - n_2) - \alpha_1(E(n) - n_2)}{n_1 - E(n)}. \tag{21}$$

After obtaining α_2, UCL_2 can be obtained using Equation (15).

Finally, by solving Equation (19), the upper warning limits are obtained as:

$$UWL_s = \Phi^{-1}\left(\frac{(2\Phi(UCL_s) - 1)\sqrt{P_0} + 1}{2}\right). \tag{22}$$

Note that, since n_1, n_2 and $E(n)$ are fixed, P_0 is obtained using Equation (16).

5. Performance measures

The average time to signal (ATS) is the most important criterion for measuring the performance of a control chart. In non-adaptive (FP) control charts or adaptive schemes with fixed sampling intervals, the average run length (ARL) can be easily converted to ATS by multiplying it by the sampling interval. However, in an adaptive scheme with varying sampling intervals (such as the VP scheme), the ATS should be separately computed.

There are two very popular methods for computing a control chart's performance measure: i) Monte Carlo simulation and ii) Markov chains. Although the simulation method is easier to perform, it takes considerable time and energy (electricity) and just gives us an approximation of the measures. The Markov chains method, on the other hand, *instantly* gives an *exact* response. These make the Markov chains a much better approach than the simulation method; especially when we are dealing with adaptive schemes. However, to use the Markov chains approach, the distributions of the used statistics in both in- and out-of-control situations should be known, and the transition probabilities should be computed. We have established the statistics in Section 3 and by computing the necessary probabilistic relations, we develop a Markov chain model to compute the performance measures. To do so, we first define the following states for the control chart:

State 1: $SS_k \in \left[0, UWL_{(k)}\right]$, State 2: $SS_k \in (UWL_{(k)}, UCL_{(k)}]$, State 3: $SS_k \in (UCL_{(k)}, \infty)$.

States 1 and 2 are transient (in-control) states, while state 3 is an absorbing (out-of-control) one. The Markov transition probability matrix is $\mathbf{P} = \begin{bmatrix} p_{11} & p_{12} & p_{13} \\ p_{21} & p_{22} & p_{23} \\ p_{31} & p_{32} & p_{33} \end{bmatrix}$, where, for instance, p_{12} is the probability of transition from state 1 to state 2.

The transition probabilities p_{11}, p_{12}, p_{21}, and p_{22} for the proposed max-type control chart can be computed as:

$$\begin{aligned} p_{s1} &= P(SS_k \le UWL) \\ &= P(\max\{|ST_k{}^2|, |SV_k|\} \le UWL) \\ &= P(|ST_k{}^2| \le UWL)P(|SV_k| \le UWL), \end{aligned} \tag{23}$$

$$\begin{aligned} p_{s2} &= P(UWL < SS_k \le UCL) \\ &= P(UWL < \max\{|ST_k{}^2|, |SV_k|\} \le UCL) \\ &= P(|ST_k{}^2| \le UCL)P(|SV_k| \le UCL) \\ &\quad - P(|ST_k{}^2| \le UWL)P(|SV_k| \le UWL), \end{aligned} \tag{24}$$

where $s \in [1, 2]$. The other probabilities are simply computed as $p_{13} = 1 - p_{11} - p_{12}$, $p_{23} = 1 - p_{21} - p_{22}$, $p_{31} = p_{32} = 0$, and $p_{33} = 1$. Note that, to simplify the notations, we omit the index (k) in $UWL_{(k)}$ and $UCL_{(k)}$ from Equations (23) and (24) onward.

It is clear from Equations (23) and (24) that we only need to compute two types of terms to compute p_{s1} and p_{s2}. One type relates to $ST_k{}^2$ and the other one to SV_k.

First, for $P(|ST_k{}^2| \le UCL)$ we have:

$$\begin{aligned} P(|ST_k{}^2| \le UCL) &= P\left(\left|\Phi^{-1}\left[F_{p(q+1)}(T_k^2)\right]\right| \le UCL\right) \\ &= P(|F_{p(q+1)}(T_k^2)| \le \Phi(UCL)) \\ &= P(|T_k^2| \le F^{-1}_{p(q+1)}(\Phi(UCL))) \\ &= P\left(\left|\left(\hat{\boldsymbol{\beta}}_k - \boldsymbol{\beta}\right)\boldsymbol{\Sigma}^{-1}_{\hat{\boldsymbol{\beta}}_k}\left(\hat{\boldsymbol{\beta}}_k - \boldsymbol{\beta}\right)^T\right| \right. \\ &\quad \left. \le F^{-1}_{p(q+1)}(\Phi(UCL))\right). \end{aligned} \tag{25}$$

When the process is in-control, we have $\boldsymbol{\beta} = \boldsymbol{\beta}_0$ and $\boldsymbol{\Sigma} = \boldsymbol{\Sigma}_0$, and Equation (25) is simply computed as:

$$\begin{aligned} P(|ST_k{}^2| \le UCL) &= [F_{p(q+1)}(F^{-1}_{p(q+1)}(\Phi(UCL))) \\ &\quad - F_{p(q+1)}(F^{-1}_{p(q+1)}(\Phi(-UCL)))] \\ &= \Phi(UCL) - \Phi(-UCL). \end{aligned} \tag{26}$$

When the process is out-of-control, we have $\boldsymbol{\beta} = \boldsymbol{\beta}_1$ and $\boldsymbol{\Sigma} = \boldsymbol{\Sigma}_1$, and $T_k{}^2$ follows a non-central χ^2 distribution $T_k{}^2 \sim \chi^2(p(q+1), \lambda_1)$, where λ_1 is the non-centrality parameter and is equal to $\lambda_1 = (\boldsymbol{\beta}_1 - \boldsymbol{\beta}_0)\ \boldsymbol{\Sigma}^{-1}_{\hat{\boldsymbol{\beta}}_k}(\boldsymbol{\beta}_1 - \boldsymbol{\beta}_0)^T$.

Since $\boldsymbol{\Sigma}_{\hat{\boldsymbol{\beta}}_k}$ is related to $\boldsymbol{\Sigma}$ via Equation (4), a shift in $\boldsymbol{\Sigma}$ will affect the T_k^2 value as well. Let us assume that $\boldsymbol{\Sigma}_{\hat{\boldsymbol{\beta}}_{0k}}$ and $\boldsymbol{\Sigma}_{\hat{\boldsymbol{\beta}}_{1k}}$ are $\boldsymbol{\Sigma}_{\hat{\boldsymbol{\beta}}_k}$ when $\boldsymbol{\Sigma}$ is in- ($\boldsymbol{\Sigma}_0$) and out-of-control ($\boldsymbol{\Sigma}_1$), respectively. To be able to compute Equation (25) in an out-of-control situation, we assume that $\boldsymbol{\Sigma}_1 = \tau\boldsymbol{\Sigma}_0$ with $\tau > 0$, which results in $\boldsymbol{\Sigma}_{\hat{\boldsymbol{\beta}}_{1k}} = \tau\boldsymbol{\Sigma}_{\hat{\boldsymbol{\beta}}_{0k}}$. Note that τ is a constant that is a generalized multiplier, which shows how much the $\boldsymbol{\Sigma}$ matrix has shifted. If all the elements of $\boldsymbol{\Sigma}$ (and consequently $\boldsymbol{\Sigma}_{\hat{\boldsymbol{\beta}}_k}$) shift with an equal multiplier (τ), then $\boldsymbol{\Sigma}_1 = \tau\boldsymbol{\Sigma}_0$ holds exactly; otherwise, we will demonstrate a way to estimate τ later on in this section.

Therefore, λ_1, when there is also a shift in $\boldsymbol{\Sigma}$, changes into:

$$\lambda_1 = \frac{1}{\tau}(\boldsymbol{\beta}_1 - \boldsymbol{\beta}_0)\boldsymbol{\Sigma}^{-1}_{\hat{\boldsymbol{\beta}}_{0k}}(\boldsymbol{\beta}_1 - \boldsymbol{\beta}_0)^T. \tag{27}$$

Consequently, when the process is out-of-control, Equation (25) is computed as:

$$\begin{aligned} P(|ST_k{}^2| \le UCL) &= \left[F_{p(q+1),\lambda_1}\left(\frac{1}{\tau}F^{-1}_{p(q+1)}(\Phi(UCL))\right)\right. \\ &\quad \left. - F_{p(q+1),\lambda_1}\left(\frac{1}{\tau}F^{-1}_{p(q+1)}(\Phi(-UCL))\right)\right]. \end{aligned} \tag{28}$$

Note that, to compute $P(|ST_k{}^2| \le UWL)$, we simply replace UCL with UWL in Equations (26) and (28).

Second, for SV_k type terms, and for $P(|SV_k| \le UCL)$, we have:

$$\begin{aligned} P(|SV_k{}^2| \le UCL) &= P\left(\left|\Phi^{-1}\left[\Gamma_{\frac{n}{2},2b}(V_k)\right]\right| \le UCL\right) \\ &= P\left(\left|\Gamma_{\frac{n}{2},2b}(V_k)\right| \le \Phi(UCL)\right) \\ &= P\left(|V_k| \le \Gamma^{-1}_{\frac{n}{2},2b}(\Phi(UCL))\right) \\ &= P\left(|\mathbf{a}^T\mathbf{MSE}_{\boldsymbol{k}}\ \mathbf{a}| \le \Gamma^{-1}_{\frac{n}{2},2b}(\Phi(UCL))\right). \end{aligned} \tag{29}$$

When the process is out-of-control and the mean (B matrix) has shifted, the $V_k\ = \mathbf{a}^T\mathbf{MSE}\ \mathbf{a}$ statistic has a different distribution than $\text{Gamma}\left(\frac{n}{2}, 2b\right)$. In this case, Equation (6) is rewritten as $\mathbf{SSE}_{\boldsymbol{k}} = (\mathbf{E} + \mathbf{X}(\mathrm{B}_1 - \mathrm{B}_0))^T_{\boldsymbol{k}}(\mathbf{E} + \mathbf{X}(\mathrm{B}_1 - \mathrm{B}_0))_k$, where B_0 and B_1 are the coefficients matrices when the process is in- and out-of-control, respectively. Therefore, according to Chatfield and Collins (2000), the $\mathbf{SSE}_{\boldsymbol{k}}$ distribution changes into a non-central Wishart distribution with the non-centrality parameter $\mathbf{M}{=}\mathbf{X}(\mathrm{B}_1 - \mathrm{B}_0)$, i.e., $\mathbf{SSE}_{\boldsymbol{k}} \sim W_p(\boldsymbol{\Sigma}_1, n; \mathbf{M})$. We also have $\mathbf{a}^T\mathbf{SSE}\ \mathbf{a}\ \sim (\mathbf{a}^T\boldsymbol{\Sigma}\ _1\mathbf{a})\ \chi^2(n, \lambda_2)$, where $\lambda_2 = \frac{\mathbf{a}^T\mathbf{M}^T\mathbf{M}\ \mathbf{a}}{\mathbf{a}^T\boldsymbol{\Sigma}_1\ \mathbf{a}}$ is the non-centrality parameter of the chi-square distribution. Consequently, by letting $c = \frac{\mathrm{a}^T\boldsymbol{\Sigma}\ _1\ \mathrm{a}}{n}$, we have $V_k\ \sim c\ \chi^2(n, \lambda)$.

Hence, Equation (29) is computed as:

$$\begin{aligned} P(|SV_k{}^2| \le UCL) = \Bigg[& F_{n,\lambda_2}\left(\frac{1}{c}\Gamma^{-1}_{\frac{n}{2},2b_0}(\Phi(UCL))\right) \\ & - F_{n,\lambda_2}\left(\frac{1}{c}\Gamma^{-1}_{\frac{n}{2},2b_0}(\Phi(-UCL))\right)\Bigg], \end{aligned} \tag{30}$$

When the process is in-control, Equation (30) reduces to:

$$P(|SV_k{}^2| \le UCL) = \Phi(UCL) - \Phi(-UCL). \tag{31}$$

Similarly, to compute the $P(|SV_k{}^2| \le UWL)$ term, simply replace UCL with UWL in Equations (30) and (31).

Note that, as mentioned above, we assume that τ is a constant number, i.e., each element in the variance-covariance matrix shifts with the same multiplier (τ). In general, each element of $\boldsymbol{\Sigma}_0$ may shift independently at different rates. In such cases, as $\boldsymbol{\Sigma}_0$ and $\boldsymbol{\Sigma}_{\hat{\boldsymbol{\beta}}_{0k}}$ matrices have different dimensions (despite being interconnected), the multiplier (τ_1) in $\boldsymbol{\Sigma}_1 = \tau_1\boldsymbol{\Sigma}_0$ is going to be different from the multiplier (τ_2) in $\boldsymbol{\Sigma}_{\hat{\boldsymbol{\beta}}_{1k}} = \tau_2\boldsymbol{\Sigma}_{\hat{\boldsymbol{\beta}}_{0k}}$. However, since Equation (27) only contains $\boldsymbol{\Sigma}_{\hat{\boldsymbol{\beta}}_{0k}}$, we only need to have the τ_2 value. To compute τ_2, we can use the concept of matrix generalization to change the matrices into numbers. According to Rencher (2002), the generalized form of a variance-covariance matrix (its determinant) is called the generalized variance, and it increases/decreases if the variances increase/decrease and/or the intercorrelations decrease/increase.

To do so, we can approximate τ_2 as $\tau_2\mathbf{I} = \boldsymbol{\Sigma}_{\hat{\boldsymbol{\beta}}_{1k}}\boldsymbol{\Sigma}^{-1}_{\hat{\boldsymbol{\beta}}_{0k}} \Rightarrow \tau_2 \approx |\boldsymbol{\Sigma}_{\hat{\boldsymbol{\beta}}_{1k}}\boldsymbol{\Sigma}^{-1}_{\hat{\boldsymbol{\beta}}_{0k}}|^{1/(q+1)p}$. We have confirmed via simulation (To do that, we have computed the chart's performance with both the Monte Carlo simulation method and the proposed Markov chain model and compared the results) that this is a good approximation for τ_2. Note that, if each element of $\boldsymbol{\Sigma}_{\hat{\boldsymbol{\beta}}_{0k}}$ shifts with an equal multiplier, then the above formula is not an approximation anymore, and it will give us an exact response, i.e., $\tau = \tau_1 = \tau_2 = |\boldsymbol{\Sigma}_1\boldsymbol{\Sigma}_0^{-1}|^{1/p} = |\boldsymbol{\Sigma}_{\hat{\boldsymbol{\beta}}_{1k}}\ \boldsymbol{\Sigma}^{-1}_{\hat{\boldsymbol{\beta}}_{0k}}|^{1/(q+1)p}$.

Lastly, when we computed all the transition probabilities in both in- and out-of-control situations, we have:

$$\text{ARL} = \mathbf{b}^T(\mathbf{I}{-}\mathbf{Q})^{-1}\mathbf{1}, \tag{32}$$

$$\text{ATS} = \mathbf{b}^T(\mathbf{I}{-}\mathbf{Q})^{-1}\mathbf{t}, \tag{33}$$

where $\mathbf{b}^{\mathbf{T}}{=}(b_1, b_2)$ is the vector of starting probabilities such that $b_1 + b_2 = 1$, $\mathbf{I}$ is the identity matrix of order 2, $\mathbf{Q}$ is a 2×2 transition probability matrix for the transient states, $\mathbf{1}$ is a 2×1 unit column vector and $\mathbf{t} = (t_1, t_2)^T$ is the vector of sample sizes.At the beginning, when the process is assumed to be in-control ($\mathrm{B} = \mathrm{B}_0\ \&\ \boldsymbol{\Sigma} = \boldsymbol{\Sigma}_0$), b_1 and b_2 are obtained as $b_1 = \frac{p_{11}}{p_{11}+p_{12}}$ and $b_2 = \frac{p_{22}}{p_{21}+p_{22}}$.

6. Numerical analyses

In this section, we compare the performance of our proposed control charts with some of the best available control charts. We also evaluate the performance of the proposed control charts under different shift scenarios and different dimensions. Note that, in this research we consider separate and simultaneous step (sustained) shifts in the parameters (intercepts, slopes, and error's variance-covariance matrix) and increase the shift sizes until we get a near one ARL/ATS. Since it is not feasible to consider all the possible shift size

Table 1. ATS comparisons with other charts for shifts in the $\boldsymbol{\beta}_0 = (\beta_{01}, \beta_{02})$ vector, when $p = 2$, $q = 2$, and $\rho = 0.5$.

Shift in $\boldsymbol{\beta}_0$	ELRT	Max-MEWMA	Max-MCUSUM	Proposed Max-VP chart	Proposed Max-FP chart	FP chart with only T^2 statistic	FP chart with only V statistic
(0.2,0.4)	29.35	37.10	**13.19**	100.19	133.01	139.75	139.75
(0.2,0.6)	13.44	13.54	**8.58**	39.04	81.97	80.83	103.84
(0.2,0.8)	8.24	7.61	**6.19**	11.03	42.27	38.45	71.84
(0.2,1)	5.82	5.26	4.49	**3.36**	20.35	17.68	47.68
(0.2,1.4)	3.51	3.34	3.38	**1.23**	5.33	4.67	20.55
(0.2,2)	2.1	2.19	2.15	**1.02**	1.53	1.47	6.73
(0.4,0.4)	22.46	25.92	**8.53**	66.87	103.79	122.02	103.84
(0.4,0.6)	13.32	13.62	**6.21**	30.13	67.30	80.83	71.84
(0.4,0.8)	8.68	8.06	**4.91**	10.23	38.02	43.08	47.68
(0.4,1)	6.19	5.66	4.09	**3.47**	20.01	21.04	31.21
(0.4,1.4)	3.83	3.53	3.04	**1.262**	5.75	5.61	13.79
(0.4,2)	2.2	2.28	2.14	**1.02**	1.62	1.61	4.92
(0.6,0.6)	10.95	10.62	**4.9**	15.76	46.04	62.12	47.68
(0.6,0.8)	8.14	7.64	**4.11**	6.59	28.22	38.45	31.21
(0.6,1)	6.29	5.7	3.52	**2.81**	16.35	21.04	20.55
(0.5,1.4)	3.85	3.61	2.87	**1.25**	5.69	5.97	11.4
(0.5,2)	2.26	2.34	2.13	**1.03**	1.65	1.68	4.26
(0.8,0.8)	6.98	6.44	**3.53**	3.56	18.8	27.98	20.55
(0.8,1)	5.76	5.27	3.07	**2.03**	11.9	17.68	13.79
(1)	5.1	4.67	2.75	**1.52**	8.19	12.91	9.49
(2)	1.98	2.1	1.42	**1.02**	1.08	1.37	1.22

The smallest numbers in all rows are bolded.

combinations, without losing generality, we randomly select the shift sizes to reduce the paper's volume.

6.1. Comparisons with other control charts

In the first part of our numerical analyses section, we compare the proposed FP and VP max-type schemes with some of the best available control charts for multivariate multiple linear profiles, namely the ELRT and Max-MEWMA, and Max-MCUSUM charts. We use the ATS for these comparisons. Since no Markov chain model has yet been developed for these control charts, the performances of the ELRT, Max-MEWMA, and Max-MCUSUM control charts are computed by using the Monte Carlo simulation method with 10,000 runs. All the comparison environments and the chosen values for the process and chart parameters are exactly the same as Eyvazian et al. (2011) and Ghashghaei and Amiri (2017a), except for our adaptive (VP) control chart, in which we had to add some other values for extra VP chart parameters (details follow). The in-control ATS for all the considered control charts is set to 200 hrs ($\alpha = 0.005$). The analysis for the first part is conducted for the case of two response variables ($p = 2$), i.e., two multiple linear profiles. The following regression models are used for the numerical analysis in this part: $y_1 = 3 + 2x_1 + x_2 + \varepsilon_1$ and $y_2 = 2 + x_1 + x_2 + \varepsilon_2$.

The error's variance-covariance matrix for this part is assumed to have the following elements: $\boldsymbol{\Sigma} = \begin{bmatrix} \sigma_1^2 & \rho\sigma_1\sigma_2 \\ \rho\sigma_1\sigma_2 & \sigma_1^2 \end{bmatrix}$, where σ_1 and σ_2 are the standard deviations of the first and second profiles, respectively, and ρ is their correlation. For its in-control value, we have: $\boldsymbol{\Sigma}_0 = \begin{bmatrix} 1 & 0.5 \\ 0.5 & 1 \end{bmatrix}$.

The sample size for ELRT, Max-MEWMA, Max-MCUSUM, and the proposed Max-Shewhart-type FP control chart is 4 and the sampling interval is 1 hr. For the proposed Max-Shewhart-type VP control chart, in which we need two types of each chart parameter, the following parameters' values are chosen: $n_1 = 4$, $n_2 = 8$, $E(n) = 6$, $E(\alpha) = 0.005$, $\alpha_1 = 0.004$, $E(t) = 1$ hr and $t_2 = 0.1$ hr. The other chart parameters are computed using Equations (15) and (20)–(22) as $t_2 = 1.9$ hrs, $UCL_1 = 3.0899$, $UWL_1 = 1.0487$, $UCL_2 = 2.9673$, and $UWL_2 = 1.0472$.

For each sample size, a set of explanatory variables is required. The $\mathbf{X}$ matrix for $n = 4$ is assumed to be $\mathbf{X} = \begin{pmatrix} 1 & 2 & 1 \\ 1 & 4 & 2 \\ 1 & 6 & 3 \\ 1 & 8 & 2 \end{pmatrix}$ and for the sample size 8 (only needed for the VP chart) it is considered $\mathbf{X} = \begin{pmatrix} 1 & 2 & 1 \\ 1 & 4 & 2 \\ 1 & 6 & 3 \\ 1 & 8 & 2 \\ 1 & 9 & 3 \\ 1 & 10 & 1 \\ 1 & 9 & 2 \\ 1 & 11 & 1 \end{pmatrix}$. It should also be noted that since the in-control standard deviations are assumed to be equal (to 1), the chart's performance remains unchanged for similar separate shifts. For example, the performance of the chart for a (0.2,0.1) shift in $\boldsymbol{\beta}_0$

Table 2. ATS comparisons with other charts for shifts in the $\boldsymbol{\beta}_1 = (\beta_{11}, \beta_{12})$ vector, when $p = 2$, $q = 2$, and $\rho = 0.5$.

Shift in $\boldsymbol{\beta}_1$	ELRT	Max-MEWMA	Max-MCUSUM	Proposed Max-VP chart	Proposed Max-FP chart	FP chart with only T^2 statistic	FP chart with only V statistic
(0.025,0.05)	57.42	86.09	**24.03**	110.63	167.07	171.34	170.28
(0.025,0.075)	26.43	33.16	**15.55**	46.06	134.70	134.58	148.84
(0.025,0.1)	15.44	15.7	**11.02**	13.63	96.71	91.43	124.52
(0.025,0.125)	10.11	9.76	8.37	**4.25**	62.75	55.83	100.09
(0.02,0.14)	8.19	7.63	7.49	**2.53**	46.15	38.88	90.84
(0.02,0.2)	4.81	4.43	4.8	**1.34**	13.42	10.97	47.18
(0.05,0.05)	44.77	63.55	**13.37**	77.09	149.61	161.76	148.843
(0.05,0.075)	26.74	33.33	**10.99**	36.40	121.86	134.58	124.52
(0.05,0.1)	16.23	17.24	**8.22**	12.78	90.02	97.51	100.09
(0.05,0.125)	11.12	10.55	6.82	**4.40**	60.94	62.87	77.89
(0.06,0.14)	9.27	8.7	5.63	**2.64**	45.15	47.89	59.27
(0.06,0.2)	5.34	4.89	4.06	**1.36**	14.89	14.23	29.66
(0.075,0.075)	21.24	24.09	**8.35**	19.60	99.93	118.41	100.09
(0.075,0.1)	15.09	15.82	**6.83**	8.36	75.23	91.43	77.89
(0.075,0.125)	10.93	10.43	5.69	**3.58**	52.76	62.87	59.27
(0.08,0.14)	9.16	8.58	5.02	**2.35**	40.12	47.89	47.18
(0.08,0.2)	5.49	4.99	3.74	**1.35**	14.39	15.27	23.57
(0.1,0.1)	12.53	12.58	5.66	**4.55**	57.91	75.58	59.28
(0.1,0.125)	10.13	9.58	4.87	**2.58**	41.95	55.83	44.53
(0.1,0.14)	8.87	8.3	4.52	**2.02**	33.84	44.61	37.41
(0.1,0.2)	5.51	5	3.44	**1.32**	13.22	15.63	18.82
(0.125,0.125)	8.83	8.32	4.29	**1.92**	31.48	44.51	33.31
(0.2,0.2)	4.5	4.15	2.54	**1.15**	5.75	9.19	6.83
(0.3,0.3)	2.55	2.59	1.77	**1.02**	1.47	2.17	1.81

The smallest numbers in all rows are bolded.

is similar to its performance for a (0.1,0.2) shift. This is valid for $\boldsymbol{\beta}_1$, $\boldsymbol{\beta}_2$ and $\boldsymbol{\sigma}$ as well. Similarly, in the case of $p = 3$ (used in Section 6.2), the chart performance for (0.2,0.1,0.1), (0.1,0.2,0.1) and (0.1,0.1,0.2) shifts are all equal. This applies to any value of p.

Tables 1 and 2 show the charts' comparisons in terms of shifts in the intercepts ($\boldsymbol{\beta}_0$ vector) and first slops ($\boldsymbol{\beta}_1$ vector), respectively. The results show that the proposed Max-Shewhart-type VP control chart performs better in detecting most moderate and large intercept and slope mean vector shifts, and the Max-MCUSUM chart performs better in detecting small shifts.

According to Table 3, for detecting shifts in errors' standard deviation ($\boldsymbol{\sigma}$ vector), the newly proposed method performs better in detecting variability shifts in most cases, and the Max-MEWMA chart performs better in other ones. Table 4 contains the performance values in the case of simultaneous shifts in both standard deviation and intercept of the first profile. Yet again, the proposed Max-Shewhart-type VP control chart performs better in most shifts, and in the other ones, ELRT and Max-MEWMA charts perform better.

As can be seen in Tables 1–4, we have also compared the performance of the proposed max-type control chart with the charts plotting only the Hotelling's T^2 statistic (Equation (5)) or our newly proposed V statistic (Equation (7)). The results show that if these two statistics are combined, forming our proposed max-type control chart via Equation (13)'s statistic, they mostly perform better, especially in detecting variability shifts (Table 3), in which it performs better in all the compared shift size cases. Although the proposed V statistic does not do a good job on its own in detecting the variability shifts (even worse than the Hotelling's T^2 statistic), when combined with the Hotelling's T^2 statistic, the max-type chart's performance gets significantly improved. Considering the mean vector shifts, the V chart performs better than the Hotelling's T^2 chart in detecting small shifts, but it still performs weaker than the max-type chart in this regard as well. As in simultaneous shifts (Table 4), the max-type control chart performs better in most cases, while the Hotelling T^2 control chart performs better in the rest (mostly when the mean shift is more significant than the variability shift).

6.2. Extensive evaluations

In this section, we first perform a more comprehensive performance evaluation of the proposed Max-Shewhart-type VP control chart using both ARL and ATS performance measures. To better and easier evaluate the chart's performance, in this section we assume that τ is a constant number, i.e., each element in the variance-covariance matrix shifts with the same multiplier (τ). We perform this analysis for the cases of $p = 2$ and 3 (two and three profiles). Also, the correlations between the responses in this section are assumed to be equal (regarding the $p = 3$ case, and later on the $p = 6$ case), and it is not fixed at $\rho = 0.5$. The other assumptions for the values of the parameters are the same as in

Table 3. ATS comparisons with other charts for shifts in the error standard deviation $\boldsymbol{\sigma} = (\sigma_1, \sigma_2)$, when $p = 2$, $q = 2$, and $\rho = 0.5$..

Shift in $\boldsymbol{\sigma}$	ELRT	Max-MEWMA	Max-MCUSUM	Proposed Max-VP chart	Proposed Max-FP chart	FP chart with only T^2 statistic	FP chart with only V statistic
(1.1,1.1)	66.31	**46.1**	106.2	63.88	79.89	84.98	95.15
(1.1,1.2)	33.98	**24.04**	72.11	33.07	48.1	52.89	62.55
(1.1,1.3)	18.87	**14.02**	44.64	17.95	30.36	34.72	41.95
(1.1,1.4)	12.11	**9.75**	27.72	10.41	20.25	24.12	29.09
(1.1,1.5)	6.68	7.72	17.47	**6.49**	14.22	17.62	20.92
(1.2,1.2)	23.63	**14.72**	48.3	17.69	29.86	33.51	42.39
(1.2,1.3)	15.48	10.42	31.11	**10.17**	19.67	22.7	29.62
(1.2,1.4)	10.81	7.81	20.16	**6.31**	13.70	16.3	21.41
(1.2,1.5)	8.16	6.16	13.95	**4.23**	10.02	12.28	16
(1.3,1.3)	12.02	8.03	21.12	**6.25**	13.53	15.89	21.57
(1.3,1.4)	9.19	6.51	15.04	**4.17**	9.81	11.76	16.21
(1.3,1.5)	7.27	5.36	11	**3.01**	7.43	9.11	12.54
(1.4,1.4)	7.54	5.44	11.47	**2.99**	7.37	8.94	12.61
(1.4,1.5)	6.38	4.72	9.07	**2.31**	5.76	7.1	10.05
(1.5,1.5)	5.54	4.18	7.44	**1.89**	4.63	5.75	8.23
(1.6,1.6)	4.34	3.54	5.37	**1.45**	3.2	4.08	5.86
(1.7,1.7)	3.62	2.95	4.29	**1.25**	2.47	3.12	4.45
(1.8,1.8)	3.03	2.6	3.59	**1.15**	2	2.52	3.56
(1.9,1.9)	2.62	2.34	3.08	**1.09**	1.71	2.13	2.96
(2)	2.35	2.11	2.7	**1.06**	1.5	1.86	2.55

The smallest numbers in all rows are bolded.

Table 4. ATS comparisons with other charts for simultaneous shifts in σ_1 and β_{01}, when $p = 2$, $q = 2$, and $\rho = 0.5$.

Shift in (σ_1, β_{01})	ELRT	Max-MEWMA	Max-MCUSUM	Proposed Max-VP chart	Proposed Max-FP chart	FP chart with only T^2 statistic	FP chart with only V statistic
(1.1,0.2)	**49.05**	58.45	50.48	99.72	118.82	119.29	135.90
(1.1,0.4)	**18.82**	20.26	22.53	51.41	83.08	76.67	117.60
(1.1,0.6)	10.11	**9.7**	12.4	17.82	47.28	40.3	93.23
(1.1,0.8)	6.67	6.18	8.12	**5.52**	24.16	19.79	68.87
(1.1,1)	4.86	4.57	5.78	**2.24**	12.24	10.03	48.51
(1.1,1.5)	2.85	2.82	3.14	**1.11**	3.02	2.67	18.9
(1.1,2)	1.93	2.07	2.11	**1.02**	1.38	1.33	7.9
(1.3,0.2)	**16.42**	16.95	33.01	28.20	44.71	49.74	58.32
(1.3,0.4)	**11.02**	11.34	17.64	16.19	32.86	33.92	51.07
(1.3,0.6)	7.64	7.54	10.73	**7.24**	20.99	20.19	41.69
(1.3,0.8)	5.06	5.49	7.32	**3.18**	12.53	11.56	32.38
(1.3,1)	4.32	4.23	5.28	**1.76**	7.43	6.76	24.39
(1.3,1.5)	2.65	2.72	3.01	**1.09**	2.49	2.34	11.57
(1.3,2)	1.86	1.99	2.04	**1.01**	1.3	1.3	5.78
(1.5,0.2)	8.21	**7.99**	16.83	9.43	19.71	24.47	27.12
(1.5,0.4)	6.93	6.77	11.67	**6.33**	15.66	18.15	24.55
(1.5,0.6)	5.66	5.54	8.23	**3.65**	11.19	12.09	21.05
(1.5,0.8)	4.53	4.51	6.16	**2.15**	7.56	7.761	17.37
(1.5,1)	3.73	3.72	4.7	**1.49**	5.03	5.04	13.97
(1.5,1.5)	2.46	2.54	2.85	**1.08**	2.14	2.11	7.8
(1.5,2)	1.79	1.92	2.02	**1.01**	1.28	1.28	4.48
(1.8,0.2)	4.56	4.32	7.32	**3.04**	8.05	11.39	11.3
(1.8,0.4)	4.25	4.07	6.44	**2.48**	6.96	9.27	10.62
(1.8,0.6)	3.83	3.73	5.34	**1.91**	5.60	6.95	9.64
(1.8,0.8)	3.37	3.35	4.57	**1.50**	4.32	5.04	8.51
(1.8,1)	2.97	2.98	3.78	**1.27**	3.28	3.66	7.37
(1.8,1.5)	2.17	2.28	2.58	**1.06**	1.79	1.87	4.94
(1.8,2)	1.69	1.8	1.9	**1.01**	1.22	1.25	3.33
(2,0.2)	3.5	4.55	5.6	**1.96**	5.23	7.86	7.33
(2,0.4)	3.34	4.33	4.72	**1.75**	4.69	6.68	7
(2,0.6)	3.09	4.04	4.17	**1.51**	3.98	5.29	6.52
(2,0.8)	2.87	3.69	3.62	**1.31**	3.26	4.06	5.94
(1, 2)	2.57	3.34	3.24	**1.19**	2.64	3.11	5.32
(2,1.5)	2.01	2.66	2.37	**1.05**	1.62	1.76	3.9
(2)	1.62	2.12	1.82	**1.01**	1.19	1.24	2.84

The smallest numbers in all rows are bolded.

Section 6.1. The results for $p = 2$ are presented in Tables 5 (which contains simultaneous shifts in the variability and the intercepts), 6 (which contains simultaneous shifts in the variability and the first slopes), and 7 (which contains simultaneous shifts in the variability and the second slopes).

Tables 5–7 show the following in terms of both ATS and ARL performance measures:

Table 5. The ARL (first value) and ATS (second value) of the adaptive control chart for shifts in the intercept vector ($\boldsymbol{\beta}_0$) and the error variation (τ), when $p = 2$ and $q = 2$.

Shift in $\boldsymbol{\beta}_0 = (\beta_{01}, \beta_{02})$						
	(0,0)	(0.2,0)	(0.2,0.2)	(0.5,0.5)	(1)	(2)
τ				$\rho = 0$		
1	200, 200	178.9722, 176.7206	145.2209, 139.8380	21.4750, 14.2991	1.7883, 1.1401	1.0019, 1.0002
1.1	130.0189, 123.5655	110.7502, 103.2103	85.3733, 76.7863	14.2714, 8.7030	1.7041, 1.1256	1.0022, 1.0002
1.3	45.8362, 37.4279	39.3997, 31.3290	31.2142, 23.7316	7.6995, 4.1748	1.5737, 1.1025	1.0027, 1.0003
1.6	13.6701, 8.7099	12.3616, 7.7023	10.5748, 6.3647	4.2092, 2.1914	1.4375, 1.0776	1.0032, 1.0003
2	5.1617, 2.7620	4.8776, 2.6004	4.4619, 2.3712	2.6083, 1.4731	1.3186, 1.0555	1.0037, 1.0004
3	1.8807, 1.2154	1.8505, 1.2059	1.8031, 1.1914	1.5218, 1.1108	1.1629, 1.0268	1.0039, 1.0004
τ				$\rho = 0.1$		
1	200, 200	179.3709, 177.1656	150.0528, 145.0704	25.6382, 17.9068	1.9930, 1.1888	1.0049, 1.0005
1.1	130.0189, 123.5655	111.1161, 103.5981	88.6759, 80.1901	16.6356, 10.5917	1.8744, 1.1664	1.0053, 1.0005
1.3	45.8362, 37.4279	39.5278, 31.4501	32.2567, 24.6865	8.6304, 4.8068	1.6970, 1.1321	1.0059, 1.0006
1.6	13.6701, 8.7099	12.3898, 7.7237	10.8088, 6.5373	4.5349, 2.3671	1.5197, 1.0969	1.0064, 1.0007
2	5.1617, 2.7620	4.8841, 2.6040	4.5180, 2.4017	2.7266, 1.5222	1.3710, 1.0673	1.0067, 1.0007
3	1.8807, 1.2154	1.8512, 1.2061	1.8098, 1.1934	1.5448, 1.1170	1.1843, 1.0310	1.0063, 1.0007
τ				$\rho = 0.5$		
1	200, 200	175.5645, 173.0292	163.2730, 159.4594	43.0301, 33.9876	3.1177, 1.5251	1.0430, 1.0044
1.1	130.0189, 123.5655	108.2626, 100.6353	98.1758, 90.0384	26.2116, 18.8015	2.7595, 1.4264	1.0415, 1.0043
1.3	45.8362, 37.4279	38.6696, 30.6517	35.2783, 27.4758	12.1547, 7.3873	2.2845, 1.2987	1.0385, 1.0040
1.6	13.6701, 8.7099	12.2217, 7.5961	11.4738, 7.0323	5.6731, 3.0265	1.8768, 1.1929	1.0345, 1.0037
2	5.1617, 2.7620	4.8481, 2.5836	4.6743, 2.4876	3.1116, 1.6913	1.5806, 1.1196	1.0299, 1.0034
3	1.8807, 1.2154	1.8473, 1.2049	1.8278, 1.1989	1.6136, 1.1359	1.2608, 1.0472	1.0211, 1.0026
τ				$\rho = 0.9$		
1	200, 200	108.6074, 101.6412	171.0735, 167.9992	59.7244, 50.3333	4.7774, 2.2167	1.1163, 1.0126
1.1	130.0189, 123.5655	65.1161, 56.7587	104.1610, 96.2831	35.2316, 27.0537	3.9697, 1.9041	1.1088, 1.0119
1.3	45.8362, 37.4279	25.7787, 18.9923	37.2047, 29.2695	15.2510, 9.8288	2.9981, 1.5556	1.0960, 1.0109
1.6	13.6701, 8.7099	9.4934, 5.6022	11.8885, 7.3443	6.5841, 3.5952	2.2597, 1.3161	1.0810, 1.0095
2	5.1617, 2.7620	4.2239, 2.2449	4.7696, 2.5404	3.3946, 1.8237	1.7819, 1.1769	1.0658, 1.0081
3	1.8807, 1.2154	1.7762, 1.1832	1.8386, 1.2022	1.6591, 1.1487	1.3239, 1.0614	1.0415, 1.0054

Table 6. The ARL (first value) and ATS (second value) of the adaptive control chart for shifts in the first slope vector ($\boldsymbol{\beta}_1$) and the error variation (τ), when $p = 2$ and $q = 2$.

Shift in $\boldsymbol{\beta}_1 = (\beta_{11}, \beta_{12})$						
	(0,0)	(0.025,0)	(0.025,0.025)	(0.05,0.05)	(0.1,0.1)	(0.2,0.2)
τ				$\rho = 0$		
1	200, 200	182.3198, 180.5162	152.9707, 148.5526	52.3986, 43.9034	3.7750, 2.0282	1.3387, 1.0609
1.1	130.0189, 123.5655	113.3739, 106.0521	90.3468, 82.1391	31.1891, 23.7926	3.2922, 1.8181	1.3172, 1.0569
1.3	45.8362, 37.4279	40.1136, 32.0313	32.5195, 25.0066	13.7840, 8.8270	2.6654, 1.5532	1.2786, 1.0496
1.6	13.6701, 8.7099	12.4773, 7.7975	10.8073, 6.5546	6.1461, 3.3665	2.1385, 1.3416	1.2306, 1.0405
2	5.1617, 2.7620	4.9007, 2.6152	4.5141, 2.4042	3.2749, 1.7823	1.7595, 1.2015	1.1813, 1.0312
3	1.8807, 1.2154	1.8544, 1.2074	1.8129, 1.1950	1.6539, 1.1498	1.3456, 1.0726	1.1043, 1.0170
τ				$\rho = 0.1$		
1	200, 200	182.6283, 180.8587	157.3407, 153.2748	59.7440, 51.1672	4.4616, 2.3436	1.3731, 1.0764
1.1	130.0189, 123.5655	113.6833, 106.3785	93.4517, 85.3350	35.1332, 27.4441	3.7910, 2.0335	1.3507, 1.0708
1.3	45.8362, 37.4279	40.2283, 32.1390	33.5102, 25.9124	15.0966, 9.8730	2.9562, 1.6663	1.3098, 1.0610
1.6	13.6701, 8.7099	12.5033, 7.8171	11.0287, 6.7171	6.5176, 3.5992	2.2911, 1.3939	1.2577, 1.0491
2	5.1617, 2.7620	4.9067, 2.6184	4.5666, 2.4325	3.3861, 1.8340	1.8369, 1.2246	1.2032, 1.0372
3	1.8807, 1.2154	1.8550, 1.2076	1.8187, 1.1968	1.6703, 1.1543	1.3679, 1.0777	1.1168, 1.0197
τ				$\rho = 0.5$		
1	200, 200	179.1617, 177.0985	169.0718, 166.0085	85.3214, 77.0900	8.2358, 4.5507	1.4956, 1.1501
1.1	130.0189, 123.5655	111.0681, 103.6683	102.2250, 94.4119	49.0288, 40.6919	6.3420, 3.4025	1.4689, 1.1350
1.3	45.8362, 37.4279	39.4404, 31.4076	36.3450, 28.5225	19.5719, 13.5714	4.2900, 2.2823	1.4187, 1.1108
1.6	13.6701, 8.7099	12.3484, 7.6998	11.6534, 7.1799	7.7158, 4.3799	2.9191, 1.6362	1.3523, 1.0845
2	5.1617, 2.7620	4.8737, 2.5998	4.7122, 2.5116	3.7271, 1.9979	2.1281, 1.3182	1.2798, 1.0608
3	1.8807, 1.2154	1.8516, 1.2065	1.8345, 1.2015	1.7176, 1.1675	1.4421, 1.0953	1.1599, 1.0296
τ				$\rho = 0.9$		
1	200, 200	116.5308, 110.4421	175.8420, 173.3955	104.7928, 97.3034	13.5537, 8.4202	1.3387, 1.0609
1.1	130.0189, 123.5655	70.0165, 61.9685	107.6349, 100.0411	60.0067, 51.4644	9.6473, 5.5979	1.3172, 1.0569
1.3	45.8362, 37.4279	27.1835, 20.3375	38.1242, 30.1735	23.0168, 16.5258	5.8026, 3.1286	1.2786, 1.0496
1.6	13.6701, 8.7099	9.7746, 5.8250	12.0396, 7.4688	8.5827, 4.9693	3.5400, 1.9148	1.2306, 1.0405
2	5.1617, 2.7620	4.2924, 2.2867	4.8006, 2.5602	3.9596, 2.1142	2.3846, 1.4096	1.1813, 1.0312
3	1.8807, 1.2154	1.7898. 1.1881	1.8439, 1.2043	1.7475, 1.1760	1.4984, 1.1091	1.1043, 1.0170

Table 7. The ARL (first value) and ATS (second value) of the adaptive control chart for shifts in the second slope vector ($\boldsymbol{\beta}_2$) and the error variation (τ), when $p = 2$ and $q = 2$.

Shift in $\boldsymbol{\beta}_2 = (\beta_{21}, \beta_{22})$	(0,0)	(0.1,0)	(0.1,0.1)	(0.2,0.2)	(0.5,0.5)	(0.8,0.8)
τ				$\rho = 0$		
1	200, 200	175.0966, 172.3560	136.1983, 129.8456	38.3539, 29.1024	1.5225, 1.0649	1.0020, 1.0002
1.1	130.0189, 123.5655	107.8226, 100.0617	79.9279, 71.0247	23.9275, 16.5303	1.4617, 1.0584	1.0023, 1.0002
1.3	45.8362, 37.4279	38.6001, 30.5503	29.7840, 22.3662	11.4733, 6.7777	1.3699, 1.0482	1.0028, 1.0003
1.6	13.6701, 8.7099	12.2279, 7.5939	10.3099, 6.1549	5.4797, 2.8811	1.2777, 1.0374	1.0035, 1.0004
2	5.1617, 2.7620	4.8503, 2.5835	4.4011, 2.3342	3.0360, 1.6468	1.2002, 1.0277	1.0040, 1.0004
3	1.8807, 1.2154	1.8461, 1.2043	1.7922, 1.1874	1.5882, 1.1269	1.0277, 1.0145	1.0043, 1.0005
τ				$\rho = 0.1$		
1	200, 200	175.5917, 172.9096	141.5710, 135.6543	44.1289, 34.5889	1.7047, 1.0948	1.0053, 1.0005
1.1	130.0189, 123.5655	108.2463, 100.5117	83.4379, 74.6341	27.1087, 19.3470	1.6141, 1.0839	1.0058, 1.0006
1.3	45.8362, 37.4279	38.7422, 30.6851	30.8803, 23.3682	12.6260, 7.6569	1.4813, 1.0673	1.0065, 1.0007
1.6	13.6701, 8.7099	12.2585, 7.6174	10.5578, 6.3377	5.8406, 3.1000	1.3527, 1.0504	1.0071, 1.0007
2	5.1617, 2.7620	4.8574, 2.5874	4.4614, 2.3671	3.1544, 1.7011	1.2484, 1.0361	1.0075, 1.0008
3	1.8807, 1.2154	1.8469, 1.2046	1.7997, 1.1897	1.6090, 1.1328	1.1227, 1.0179	1.0070, 1.0008
τ				$\rho = 0.5$		
1	200, 200	171.2937, 168.2367	156.5503, 151.9474	65.6663, 55.8329	2.7000, 1.3266	1.0537, 1.0055
1.1	130.0189, 123.5655	105.0892, 97.2336	93.7139, 85.2743	38.8666, 30.2094	2.4071, 1.2662	1.0519, 1.0053
1.3	45.8362, 37.4279	37.8008, 29.8093	34.0993, 26.3370	16.6865, 10.9075	2.0184, 1.1877	1.0483, 1.0050
1.6	13.6701, 8.7099	12.0748, 7.4777	11.2678, 6.8669	7.0301, 3.8579	1.6866, 1.1226	1.0431, 1.0046
2	5.1617, 2.7620	4.8179, 2.5650	4.6300, 2.4602	3.5218, 1.8769	1.4487, 1.0774	1.0369, 1.0041
3	1.8807, 1.2154	1.8424, 1.2031	1.8203, 1.1962	1.6693, 1.1502	1.1985, 1.0320	1.0253, 1.0030
τ				$\rho = 0.9$		
1	200, 200	98.4733, 90.6843	165.5718, 161.8275	83.7579, 74.3206	4.1352, 1.8338	1.1743, 1.0186
1.1	130.0189, 123.5655	59.3586, 50.8241	100.3228, 92.1694	48.8269, 39.7957	3.4756, 1.6261	1.1607, 1.0174
1.3	45.8362, 37.4279	24.1733, 17.5130	36.1838, 28.2787	19.9632, 13.6621	2.6696, 1.3894	1.1382, 1.0154
1.6	13.6701, 8.7099	9.1664, 5.3544	11.7145, 7.2037	7.9174, 4.4534	2.0489, 1.2238	1.1126, 1.0130
2	5.1617, 2.7620	4.1439, 2.1982	4.7332, 2.5178	3.7768, 2.0046	1.6460, 1.1268	1.0881, 1.0106
3	1.8807, 1.2154	1.7611, 1.1779	1.8325, 1.2000	1.7077, 1.1616	1.2640, 1.0455	1.0518, 1.0066

1. As the coefficients (intercepts or slops)' shift size increases, i.e., goes from (0,0) to (0.2,0.2) to, …, to (2) in Table 5 and similarly in other tables, the chart signals faster.
2. As the number of profiles their coefficients shift increases (assuming the same shift size), i.e., they go from (0.2,0) to (0.2,0.2) in Table 1 and similarly in other tables, for any variation shift size (τ), the chart signals faster at first, but as the correlation between the response variables increases, the chart signals slower. For instance, comparing the cases of (0.2,0) & (0.2,0.2) mean shifts in Table 1, with τ=1.1, for ρ=0 the ATSs are 103.21 & 76.79; for ρ=0.1 the ATSs are 103.6 & 80.2; for ρ=0.5 the ATSs are 100,63 & 90.04; and for ρ=0 .9 the ATSs are 56.76 & 96.28.
3. As the variation shift (τ) increases, i.e., τ goes from 1 to 1.1 to, …, to 3, the chart signals faster.
4. As the correlation between the response variables (ρ) increases, i.e., goes from 0 to 0.1 to 0.5 to 0.9, i) if both coefficients (β_{01} & β_{02} in Table 5, β_{11} & β_{12} in Table 6, and β_{21} & β_{22} in Table 7) shift together, the chart signals slower; ii) if only one of them shifts, the chart signals a little bit slower at first ($\rho = 0.1$), but as the correlation increases ($\rho > 0.1$) the chart signals faster; and iii) if there is no shift in the coefficients, the chart's performance does not change.

The results for the case $p = 3$ are not reported in this paper, due to similarity of the conclusions to the case $p = 2$, and to reduce the number of tables.

In addition, inspired by a real case used by Eyvazian et al. (2011), and to test our proposed control chart in larger dimensions, we perform a similar analysis for the case of $p = 6$ and $q = 6$ as well. The X matrix for this analysis (Table 11) and other chart parameters can be found in the next section. Unlike the previous cases, for this analysis, we only use the ATS performance measure and both FP and VP control charts. The results of this analysis are shown in Tables 8–10. The previous conclusions for the cases of $p = 2$ & $q = 2$ and $p = 3$ & $q = 2$ are also valid for this case.

Moreover, comparing the ATS values of the VP charts, we can conclude that in the case of only variability shifts, the proposed control chart performs better (signal faster) in higher dimensions. However, in the case of mean shifts, the situation is different depending on whether the mean shift is in the intercept vector or the slope vectors. In most cases, the larger the intercept shift is, the worse the chart performs in higher dimensions. On the contrary, the larger the slope shifts are, the better the chart

Table 8. The ATS of the FP (first value) and VP (second value) control charts for shifts in the intercept vector ($\boldsymbol{\beta}_0$) and the error variation (τ), when $p = 6$ and $q = 6$.

Shift in $\boldsymbol{\beta}_0 = (\beta_{01}, \beta_{02}, ..., \beta_{06})$						
	(0,..,0)	(0.2,0, … ,0)	(0.2, … ,0,2)	(0.5, … ,0.5)	(1, … ,1)	(2, … ,2)
τ				$\rho = 0$		
1	200, 200	199.9535, 199.9301	199.0752, 198.8238	193.9494, 192.0355	172.8812, 161.8646	90.0505, 54.7944
1.1	94.5541, 80.7207	94.4853, 80.6154	93.7537, 79.5669	89.6388, 73.7168	76.1897, 55.6722	40.1879, 17.8519
1.3	15.5467, 7.9766	15.5381, 7.9675	15.4662, 7.8879	15.0514, 7.4412	13.6739, 6.0767	9.5089, 3.0453
1.6	3.2602, 1.4707	3.2594, 1.4703	3.2530, 1.4669	3.2153, 1.4473	3.0859, 1.3851	2.6429, 1.2226
2	1.4184, 1.0495	1.4183, 1.0495	1.4174, 1.0493	1.4120, 1.0481	1.3934, 1.0441	1.3263, 1.0319
3	1.0110, 1.0009	1.0110, 1.0009	1.0110, 1.0009	1.0108, 1.0009	1.0103, 1.0008	1.0086, 1.0007
τ				$\rho = 0.1$		
1	200, 200	199.9597, 199.9366	199.3854, 199.2202	196.0356, 194.8467	182.6622, 176.1117	122.9162, 92.5779
1.1	94.5541, 80.7207	94.4875, 80.6180	94.0199, 79.9501	91.2539, 75.9963	81.9236, 63.1490	53.0798, 29.3908
1.3	15.5467, 7.9766	15.5381, 7.9676	15.4930, 7.9174	15.2144, 7.6148	14.2667, 6.6415	11.1257, 4.0312
1.6	3.2602, 1.4707	3.2594, 1.4703	3.2554, 1.4681	3.2301, 1.4549	3.1424, 1.4113	2.8260, 1.2812
2	1.4184, 1.0495	1.4183, 1.0495	1.4177, 1.0494	1.4141, 1.0486	1.4016, 1.0459	1.3547, 1.0367
3	1.0110, 1.0009	1.0110, 1.0009	1.0110, 1.0009	1.0109, 1.0009	1.0106, 1.0009	1.0093, 1.0007
τ				$\rho = 0.5$		
1	200, 200	199.9507, 199.9152	199.7376, 199.6680	198.3365, 197.8721	193.0357, 190.7868	168.5628, 155.5528
1.1	94.5541, 80.7207	94.4546, 80.5654	94.3249, 80.3897	93.1284, 78.6691	88.9539, 72.7568	73.8514, 52.7231
1.3	15.5467, 7.9766	15.5333, 7.9627	15.5236, 7.9511	15.4033, 7.8191	14.9822, 7.3683	13.4289, 5.8533
1.6	3.2602, 1.4707	3.2589, 1.4701	3.2581, 1.4696	3.2473, 1.4639	3.2089, 1.4441	3.0622, 1.3744
2	1.4184, 1.0495	1.4182, 1.0495	1.4181, 1.0495	1.4166, 1.0491	1.4111, 1.0479	1.3899, 1.0434
3	1.0110, 1.0009	1.0110, 1.0009	1.0110, 1.0009	1.0110, 1.0009	1.0108, 1.0009	1.0103, 1.0008
τ				$\rho = 0.9$		
1	200, 200	199.7819, 199.6061	199.8332, 199.7891	198.9478, 198.6603	195.6612, 194.3466	180.9232, 173.5937
1.1	94.5541, 80.7207	94.0848, 79.9852	94.4082, 80.5100	93.6449, 79.4105	90.9585, 75.5778	80.8520, 61.7261
1.3	15.5467, 7.9766	15.4825, 7.9103	15.5320, 7.9604	15.4553, 7.8759	15.1846, 7.5829	14.1566, 6.5341
1.6	3.2602, 1.4707	3.2538, 1.4678	3.2589, 1.4700	3.2520, 1.4664	3.2274, 1.4535	3.1320, 1.4064
2	1.4184, 1.0495	1.4175, 1.0493	1.4182, 1.0495	1.4172, 1.0493	1.4138, 1.0485	1.4001, 1.0455
3	1.0110, 1.0009	1.0110, 1.0009	1.0110, 1.0009	1.0110, 1.0009	1.0109, 1.0009	1.0105, 1.0009

Table 9. The ATS of the FP (first value) and VP (second value) control charts for shifts in the first slope vector ($\boldsymbol{\beta}_1$) and the error variation (τ), when $p = 6$ and $q = 6$.

Shift in $\boldsymbol{\beta}_1 = (\beta_{11}, \beta_{12}, ..., \beta_{16})$						
	(0, … ,0)	(0.025,0, … ,0)	(0.025, … ,0.025)	(0.05, … ,0.05)	(0.1, … ,0.1)	(0.2, … ,0.2)
τ				$\rho = 0$		
1	200, 200	197.1587, 195.4585	133.6811, 106.8006	29.1245, 8.0760	1.9225, 1.0439	1.0000, 1.0000
1.1	94.5541, 80.7207	90.6837, 74.8658	57.5434, 34.0440	15.9256, 3.7263	1.6972, 1.0340	1.0000, 1.0000
1.3	15.5467, 7.9766	15.0623, 7.4777	11.6453, 4.4077	5.5665, 1.5579	1.3766, 1.0196	1.0000, 1.0000
1.6	3.2602, 1.4707	3.2126, 1.4485	2.8816, 1.3016	2.0988, 1.1034	1.1389, 1.0079	1.0000, 1.0000
2	1.4184, 1.0495	1.4117, 1.0482	1.3631, 1.0383	1.2348, 1.0192	1.0342, 1.0021	1.0000, 1.0000
3	1.0110, 1.0009	1.0108, 1.0009	1.0095, 1.0008	1.0061, 1.0004	1.0009, 1.0001	1.0000, 1.0000
τ				$\rho = 0.1$		
1	200, 200	197.5021, 195.7994	156.7809, 138.6952	55.1560, 23.9471	4.0571, 1.1785	1.0017, 1.0001
1.1	94.5541, 80.7207	90.8013, 74.9906	67.9137, 45.6024	26.7202, 8.6998	3.1531, 1.1228	1.0015, 1.0001
1.3	15.5467, 7.9766	15.0641, 7.4821	12.7966, 5.3107	7.5353, 2.1549	2.0373, 1.0598	1.0010, 1.0001
1.6	3.2602, 1.4707	3.2124, 1.4487	2.9998, 1.3480	2.3922, 1.1592	1.3495, 1.0213	1.0005, 1.0001
2	1.4184, 1.0495	1.4116, 1.0482	1.3808, 1.0416	1.2856, 1.0258	1.0837, 1.0053	1.0001, 1.0000
3	1.0110, 1.0009	1.0108, 1.0009	1.0100, 1.0008	1.0075, 1.0006	1.0022, 1.0001	1.0000, 1.0000
τ				$\rho = 0.5$		
1	200, 200	196.6546, 193.5767	183.0123, 176.6971	124.2904, 94.6252	22.8490, 5.4416	1.5800, 1.0272
1.1	94.5541, 80.7207	88.9608, 72.0818	82.1425, 63.4925	53.6402, 30.0523	13.0825, 2.8279	1.4446, 1.0216
1.3	15.5467, 7.9766	14.8005, 7.2246	14.2891, 6.6679	11.1919, 4.0859	4.9482, 1.4246	1.2457, 1.0129
1.6	3.2602, 1.4707	3.1851, 1.4371	3.1445, 1.4125	2.8332, 1.2842	1.9939, 1.0875	1.0922, 1.0052
2	1.4184, 1.0495	1.4077, 1.0474	1.4019, 1.0459	1.3558, 1.0369	1.2156, 1.0171	1.0228, 1.0014
3	1.0110, 1.0009	1.0107, 1.0009	1.0106, 1.0009	1.0093, 1.0007	1.0056, 1.0004	1.0006, 1.0000
τ				$\rho = 0.9$		
1	200, 200	176.3784, 147.8113	189.5984, 186.0572	152.5101, 132.6242	48.7483, 19.3831	3.4094, 1.1323
1.1	94.5541, 80.7207	70.0504, 44.7820	86.4848, 69.3652	65.8896, 43.2422	24.1647, 7.3111	2.7286, 1.0938
1.3	15.5467, 7.9766	12.3443, 5.0462	14.7320, 7.1116	12.5771, 5.1289	7.1102, 2.0021	1.8583, 1.0478
1.6	3.2602, 1.4707	2.9245, 1.3336	3.1859, 1.4326	2.9777, 1.3390	2.3331, 1.1465	1.2962, 1.0176
2	1.4184, 1.0495	1.3696, 1.0404	1.4078, 1.0472	1.3775, 1.0410	1.2756, 1.0244	1.0715, 1.0045
3	1.0110, 1.0009	1.0098, 1.0008	1.0107, 1.0009	1.0099, 1.0008	1.0072, 1.0005	1.0019, 1.0001

Table 10. The ATS of the FP (first value) and VP (second value) control charts for shifts in the second slope vector ($\boldsymbol{\beta}_2$) and the error variation (τ), when $p = 6$ and $q = 6$.

Shift in $\boldsymbol{\beta}_2 = (\beta_{21}, \beta_{22}, \ldots, \beta_{26})$						
	(0, … ,0)	(0.1,0, … ,0)	(0.1, … ,0.1)	(0.2, … ,0.2)	(0.5, … ,0.5)	(0.8, … ,0.8)
τ				$\rho = 0$		
1	200, 200	195.3694, 192.1372	98.8919, 61.9434	12.1678, 2.1542	1.0046, 1.0003	1.0000, 1.0000
1.1	94.5541, 80.7207	88.5310, 71.4102	43.5892, 19.9435	7.8228, 1.5966	1.0038, 1.0002	1.0000, 1.0000
1.3	15.5467, 7.9766	14.7938, 7.1863	9.9555, 3.2284	3.6127, 1.1994	1.0024, 1.0001	1.0000, 1.0000
1.6	3.2602, 1.4707	3.1859, 1.4354	2.6952, 1.2345	1.7371, 1.0538	1.0010, 1.0001	1.0000, 1.0000
2	1.4184, 1.0495	1.4078, 1.0473	1.3345, 1.0330	1.1663, 1.0118	1.0003, 1.0000	1.0000, 1.0000
3	1.0110, 1.0009	1.0107, 1.0009	1.0088, 1.0007	1.0043, 1.0003	1.0000, 1.0000	1.0000, 1.0000
τ				$\rho = 0.1$		
1	200, 200	195.9006, 192.6491	130.4158, 100.0514	26.7445, 6.4040	1.1153, 1.0061	1.0000, 1.0000
1.1	94.5541, 80.7207	88.7061, 71.5887	56.1706, 31.7583	14.8635, 3.1615	1.0903, 1.0049	1.0000, 1.0000
1.3	15.5467, 7.9766	14.7962, 7.1927	11.4873, 4.2185	5.3420, 1.4779	1.0515, 1.0029	1.0000, 1.0000
1.6	3.2602, 1.4707	3.1855, 1.4357	2.8648, 1.2917	2.0616, 1.0947	1.0199, 1.0012	1.0000, 1.0000
2	1.4184, 1.0495	1.4078, 1.0474	1.3606, 1.0376	1.2280, 1.0182	1.0051, 1.0003	1.0000, 1.0000
3	1.0110, 1.0009	1.0107, 1.0009	1.0095, 1.0007	1.0060, 1.0004	1.0002, 1.0000	1.0000, 1.0000
τ				$\rho = 0.5$		
1	200, 200	194.2775, 188.1126	171.9901, 159.5462	87.5589, 50.1098	3.6523, 1.1405	1.0661, 1.0037
1.1	94.5541, 80.7207	85.8548, 67.0057	75.6988, 54.5241	39.2332, 16.4356	2.8893, 1.0995	1.0520, 1.0029
1.3	15.5467, 7.9766	14.3928, 6.7980	13.6226, 5.9850	9.3805, 2.9137	1.9271, 1.0505	1.0299, 1.0017
1.6	3.2602, 1.4707	3.1433, 1.4176	3.0810, 1.3808	2.6276, 1.2145	1.3170, 1.0186	1.0117, 1.0007
2	1.4184, 1.0495	1.4017, 1.0462	1.3927, 1.0439	1.3239, 1.0312	1.0763, 1.0047	1.0030, 1.0002
3	1.0110, 1.0009	1.0106, 1.0009	1.0103, 1.0008	1.0085, 1.0006	1.0020, 1.0001	1.0001, 1.0000
τ				$\rho = 0.9$		
1	200, 200	155.8912, 104.7011	182.9882, 175.9983	124.1952, 91.9630	9.3341, 1.7001	1.5772, 1.0266
1.1	94.5541, 80.7207	58.5130, 29.8770	82.1274, 63.0470	53.6013, 29.1512	6.2898, 1.3960	1.4425, 1.0212
1.3	15.5467, 7.9766	10.8830, 3.9021	14.2876, 6.6300	11.1873, 4.0068	3.1534, 1.1493	1.2446, 1.0127
1.6	3.2602, 1.4707	2.7586, 1.2731	3.1444, 1.4108	2.8327, 1.2800	1.6361, 1.0438	1.0918, 1.0052
2	1.4184, 1.0495	1.3443, 1.0358	1.4019, 1.0458	1.3557, 1.0367	1.1458, 1.0100	1.0227, 1.0014
3	1.0110, 1.0009	1.0091, 1.0007	1.0106, 1.0009	1.0093, 1.0007	1.0038, 1.0003	1.0006, 1.0000

performs when the dimension is higher. In both mean shift cases, a larger variability shift makes the chart perform better in higher dimensions. In addition, a larger correlation between the response variables (profiles) mostly makes a "positive"/"negative" impact on the chart's performance in the case of intercept shift and a "negative"/"positive" one in the case of slope shifts; when "all the profiles shift together"/"only one profile shifts."

7. An illustrative example

To show an application of the proposed scheme in practice, we use the real case used by Eyvazian et al. (2011). It involves a calibration case for aircrafts at NASA's Langley Research Center. There are three force vectors (normal force, axial force, side force) and three moment vectors (pitching moment, rolling moment, yawing moment) as explanatory variables ($q = 6$) and six electrical measurements of them as six response variables ($p = 6$). The relationships between the response and explanatory variables can be modeled by a multivariate multiple linear regression model. The underlying model is used to model the relationship between these six dependent variables and six independent variables:

$$\begin{aligned} y_1 &= -0.05 + 10x_1 - 0.01x_2 - 0.03x_3 \\ &\quad + 0.26x_4 + 0x_5 + 0.03x_6 + \varepsilon_1, \end{aligned}$$

$$\begin{aligned} y_2 &= 0.48 + 0.24x_1 + 21.01x_2 - 0.09x_3 \\ &\quad + 0.03x_4 - 0.12x_5 + 0.01x_6 + \varepsilon_2, \end{aligned}$$

$$\begin{aligned} y_3 &= 0.37 + 0.09x_1 + 0.01x_2 + 6.81x_3 \\ &\quad + 0.04x_4 + 0.02x_5 - 0.03x_6 + \varepsilon_3, \end{aligned}$$

$$\begin{aligned} y_4 &= 0.04 + 0x_1 + 0x_2 + 0x_3 \\ &\quad + 10.53x_4 - 0.47x_5 + 0.21x_6 + \varepsilon_4, \end{aligned}$$

$$\begin{aligned} y_5 &= 0.09 - 0.021x_1 + 0x_2 + 0.01x_3 \\ &\quad + 0.02x_4 + 7x_5 - 0.34x_6 + \varepsilon_5, \end{aligned}$$

$$\begin{aligned} y_6 &= 0.09 + 0.04x_1 + 0x_2 - 0.01x_3 \\ &\quad + 0.18x_4 - 0.34x_5 + 11.46x_6 + \varepsilon_6. \end{aligned}$$

Since there are two sampling strategies in our adaptive scheme, we use $n_1 = 8$ and $n_2 = 16$, with $E(n) = 12$. Therefore, since we have two sets of sample sizes, we need two value sets for the explanatory variables as well (each value set corresponds to an observation of the response variables). We use the same value sets used by Eyvazian et al. (2011). The 16 explanatory value sets are mentioned in Table 11. The first eight value sets in Table 11 are used for the case of $n_1 = 8$ and all sixteen of them for $n_2 = 16$.

Also, the error's in-control variance-covariance matrix is estimated to be:

$$\mathbf{\Sigma}_0 = \begin{bmatrix} 99 & 14 & 17 & 22 & 18 & 15 \\ 14 & 94 & 20 & 24 & 18 & 15 \\ 17 & 20 & 91 & 27 & 11 & 22 \\ 22 & 24 & 27 & 104 & 20 & 21 \\ 18 & 18 & 11 & 20 & 101 & 19 \\ 15 & 15 & 22 & 21 & 19 & 90 \end{bmatrix}.$$

The in-control ATS value is set to 200, i.e., the average Type-I error probability is $E(\alpha) = 0.005$. Also, $\alpha_1 = 0.004$, and α_2 is computed using Equation (21) as 0.006. It is also assumed that $E(t) = 1$ hr and $t_2 = 0.1$ hr. Other chart parameters are obtained using Equations (15), (20), and (22), as $t_1 = 1.9$ hrs, $UCL_1 = 3.0899$, $UWL_1 = 1.0487$, $UCL_2 = 2.9673$, and $UWL_2 = 1.0472$.

To show how the control chart works in practice and to see when it can detect a shift, we shift the second slope of the second profile from 0.24 to 0.34, as well as the second profile's variance and covariances as:

$$\mathbf{\Sigma}_1 = \begin{bmatrix} 99 & 10 & 17 & 22 & 18 & 15 \\ 10 & 115 & 26 & 24 & 18 & 19 \\ 17 & 26 & 91 & 27 & 11 & 22 \\ 22 & 24 & 27 & 104 & 20 & 21 \\ 18 & 18 & 11 & 20 & 101 & 19 \\ 15 & 19 & 22 & 21 & 19 & 90 \end{bmatrix}.$$

Table 11. The values of the explanatory variables used in the illustrative example.

Observation	x_1	x_2	x_3	x_4	x_5	x_6
1	0	0	0	0	0	0
2	−68.5	19.2	−106.5	43.5	54	26.9
3	−62.1	19.2	−96.5	37.8	−49.7	−39.5
4	−61.7	−21.8	−97	39.6	46.9	38.7
5	−68.4	−19.3	−107.4	42.1	−54.2	−27
6	68.5	−19.3	106.6	−43.5	−53.8	−26.7
7	61.1	−22.2	94.9	−37.2	47.9	39.5
8	62.1	20.8	97.6	−39.8	−47.4	−38.7
9	0	0	0	0	0	0
10	−68.4	19.3	107.3	42	54.5	−27.2
11	−60.5	22.4	95.1	38.8	−48.9	40.3
12	−61.1	−22.3	95	37.2	47.6	−39.3
13	−68.5	−19	106.5	43.4	−54.2	27.1
14	68.7	−19.1	−107.8	−42.2	−53.4	26.5
15	61.5	−21.6	−96.7	−39.4	47.7	−39.2
16	61.6	22.4	−95.7	−37.5	−46.2	38.5

We generate 20 consecutive samples to test the control scheme. The corresponding control chart is shown in Figure 1. The chart detects the out-of-control situation in sample No.20. The control chart includes three zones, namely safe, warning, and out-of-control zones. Ten out of these 20 samples are in the safe zone and the other 9 are in the warning zone.

8. Concluding remarks

This paper proposed a new scheme for monitoring the multivariate multiple linear profiles. The proposed max-Shewhart-type control chart is capable of simultaneous monitoring of the process mean vector and variance-covariance matrix in a single control chart. The control scheme also contains a new statistic to enhance the variability shifts detection in the multivariate profiles. We also added a variable parameters (VP) adaptive feature to the proposed scheme to increase its capability, especially in detecting small to moderate shifts.

After developing the control chart, a proper Markov chain model was developed to compute the average time to signal and average run length performance measures. In the numerical analyses section, first, the performance of the control chart was compared to some of the best available control charts, namely ELRT, Max-MEWMA, and Max-MCUSUM. The results on average showed the better performance of the proposed adaptive control chart in moderate

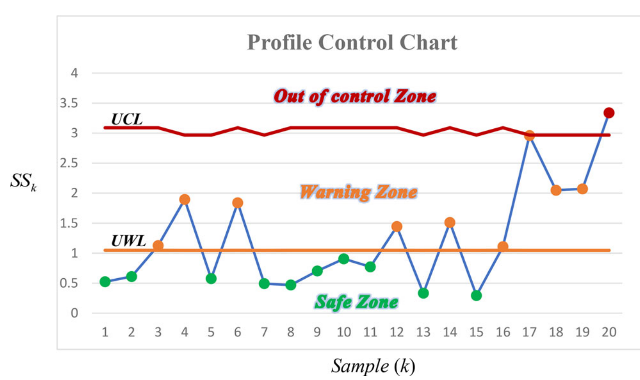

Figure 1. Profile Max-Shewhart type VP control chart.

and large shifts over all the compared control charts, especially showing very promising results in terms of variability or simultaneous shifts detection. However, the main purpose of the proposed control charts has not only been performance improvement, but most importantly, more applicability in real practice.

After comparisons with other charts, the performance of the proposed adaptive chart was extensively analyzed under small to large separate and simultaneous step shifts in the intercept and slope coefficients, and the elements of error's variance-covariance matrix, in the cases of two, three and six responses (profiles). For all response number cases, the main results are as follows: (i) as the intercept or slope coefficients shift size and/or the error's variation shift size increase, the chart signals faster; (ii) if the number of intercept or slope coefficients that shift increases from in only one profile to more than one profile, for any variation shift size (any τ value), the chart signals faster at first, but as the correlation between the response variables increases the chart signals slower; (iii) as the correlation between the response variables increases, (a) if the coefficients of all the profiles shift together, the chart signals slower, (b) if only one of them shifts, the chart signals a little bit slower at first, but as the correlation increases the chart signals faster, and (c) if there is no shift in the values of the coefficients, the chart's performance does not change; and (iv) the larger the variability shift, the better the proposed chart's performance in higher dimensions (larger p and q values).

Finally, an illustrative example based on a real case was presented to show how the proposed control chart can be easily implemented in real practice.

For future developments, investigating the separate or combined effects of measurement errors, autocorrelation and the parameters (the mean vector and the variance-covariance matrix) estimation on the performance of the proposed control chart is worth considering by researchers. One might also be interested in adding adaptive features to other available control charts for monitoring the multivariate multiple linear profiles such as ELRT, Max-MEWMA, and Max-MCUSUM charts.

About the authors

Hamed Sabahno is a Postdoc fellow at the Department of Statistics, School of Business, Economics and Statistics, Umeå University, Sweden. He has received his Ph.D., MSc, and BSc all in Industrial Engineering respectively from Shahed University and Sharif University of Technology. His main area of research is statistical process monitoring. He has published many papers in this area in high quality international journals.

Amirhossein Amiri is a Professor in Industrial Engineering at Shahed University in Iran. He holds a BS, MS, and PhD in Industrial Engineering from Khajeh Nasir University of Technology, Iran University of Science and Technology, and Tarbiat Modares University in Iran, respectively. He is now the director of Postgraduate Education at Shahed University in Iran and a member of the Iranian Statistical Association. His research interests are statistical process monitoring, profile monitoring, and change point estimation. He has published many papers in the area of statistical process control in high quality international journals such as Quality and Reliability Engineering International, Communications in Statistics, Computers and Industrial Engineering and so on. He has also published a book with John Wiley and Sons in 2011 titled Statistical Analysis of Profile Monitoring.

ORCID

Hamed Sabahno http://orcid.org/0000-0002-5618-887X
Amirhossein Amiri http://orcid.org/0000-0002-2385-8910

Acknowledgment

The authors thank the journal's editorial board and appreciate the esteemed reviewers for their constructive comments, which led to significant improvements in the quality of the paper.

References

Abdella, G., K. Yang, and A. Alaeddini. 2014. Multivariate adaptive approach for monitoring simple linear profiles. *International Journal of Data Analysis Techniques and Strategies* 6 (1):2–14. doi:10.1504/IJDATS.2014.059012.

Amiri, A., A. Saghaei, M. Mohseni, and Y. Zerehsaz. 2014. Diagnosis aids in multivariate multiple linear regression profiles monitoring. *Communications in Statistics – Theory and Methods* 43 (14):3057–79. doi:10.1080/03610926.2012.694543.

Ayoubi, M., R. B. Kazemzadeh, and R. Noorossana. 2014. Estimating multivariate linear profiles change point with a monotonic change in the mean of response variables. *The International Journal of Advanced Manufacturing Technology* 75 (9-12):1537–56. doi:10.1007/s00170-014-6208-6.

Chatfield, C., and A. J. Collins. 2000. *Introduction to multivariate analysis*. London: Chapman & Hall/CRC Press.

Chen, G., S. W. Cheng, and H. Xie. 2005. A new multivariate control chart for monitoring both location and dispersion. *Communications in Statistics – Simulation and Computation* 34 (1):203–17. doi:10.1081/SAC-200047087.

Darbani, F. H., and A. Shadman. 2018. Monitoring of linear profiles using generalized likelihood ratio control chart with variable sampling interval. *Quality and Reliability Engineering International* 34 (8):1828–35. doi:10.1002/qre.2375.

Ershadi, M. J., R. Noorossana, and S. T. A. Niaki. 2016a. Economic-statistical design of simple linear profiles with variable sampling interval. *Journal of Applied Statistics* 43 (8):1400–18. doi:10.1080/02664763.2015.1103705.

Ershadi, M. J., R. Noorossana, and S. T. A. Niaki. 2016b. Economic design of phase II simple linear profiles with variable sample size. *International Journal of Productivity and Quality Management* 18 (4):537–55. doi:10.1504/IJPQM.2016.077781.

Eyvazian, M., R. Noorossana, A. Saghaei, and A. Amiri. 2011. Phase II monitoring of multivariate multiple linear regression profiles. *Quality and Reliability Engineering International* 27 (3):281–96. doi:10.1002/qre.1119.

Fan, S.-K S., C.-H. Jen, and T.-Y. Lee. 2017. Modeling and monitoring the nonlinear profile of heat treatment process data by using an approach based on a hyperbolic tangent function. *Quality Engineering* 29 (2):226–43. doi:10.1080/08982112.2016.1193614.

Ghashghaei, R., and A. Amiri. 2017a. Maximum multivariate exponentially weighted moving average and maximum multivariate cumulative sum control charts for simultaneous monitoring of mean and variability of multivariate multiple linear regression profiles. *Scientia Iranica* 24 (5):2605–22. doi:10.24200/sci.2017.4385.

Ghashghaei, R., and A. Amiri. 2017b. Sum of squares control charts for monitoring of multivariate multiple linear regression profiles in Phase II. *Quality and Reliability Engineering International* 33 (4):767–84. doi:10.1002/qre.2055.

Ghashghaei, R., A. Amiri, and P. Khosravi. 2019. New control charts for simultaneous monitoring of the mean vector and covariance matrix of multivariate multiple linear profile. *Communications in Statistics – Simulation and Computation* 48 (5):1382–405. doi:10.1080/03610918.2017.1414246.

Jensen, W. A., G. R. Bryce, and M. R. Reynolds, Jr. 2008. Design issues for adaptive control charts. *Quality and Reliability Engineering International* 24 (4):429–45. doi:10.1002/qre.911.

Jensen, W. A., L. A. Jones-Farmer, C. W. Champ, and W. H. Woodall. 2006. Effects of parameter estimation on control chart properties: A literature review. *Journal of Quality Technology* 38 (4):349–64. doi:10.1080/00224065.2006.11918623.

Kang, L., and S. Albin. 2000. On-line monitoring when the process yields a linear. *Journal of Quality Technology* 32 (4):418–26. doi:10.1080/00224065.2000.11980027.

Kazemzadeh, R., A. Amiri, and B. Kouhestani. 2016. Monitoring simple linear profiles using variable sample size schemes. *Journal of Statistical Computation and Simulation* 86 (15):2923–45. doi:10.1080/00949655.2016.1138115.

Khedmati, M., and S. T. A. Niaki. 2016. A new control scheme for Phase II monitoring of simple linear profiles in multistage processes. *Quality and Reliability Engineering International* 32 (2):443–52. doi:10.1002/qre.1762.

Khoo, M. B. C. 2004. A new bivariate control chart to monitor the multivariate process mean and variance simultaneously. *Quality Engineering* 17 (1):109–18. doi:10.1081/QEN-200028718.

Kim, K., M. A. Mahmoud, and W. H. Woodall. 2003. On the monitoring of linear profiles. *Journal of Quality Technology* 35 (3):317–28. doi:10.1080/00224065.2003.11980225.

Li, Z., and Z. Wang. 2010. An exponentially weighted moving average scheme with variable sampling intervals for monitoring linear profiles. *Computers & Industrial Engineering* 59 (4):630–7. doi:10.1016/j.cie.2010.07.011.

Magalhaes, M. S., and R. Von Doellinger. 2016. Monitoring linear profiles using an adaptive control chart. *The International Journal of Advanced Manufacturing Technology* 82 (5-8):1433–45. doi:10.1007/s00170-015-7429-z.

Maleki, M. R., A. Amiri, and P. Castagliola. 2018. An overview on recent profile monitoring papers (2008–2018) based on conceptual classification scheme. *Computers & Industrial Engineering* 126:705–28. doi:10.1016/j.cie.2018.10.008.

Malela-Majika, J. C., K. Chatterjee, and C. Koukouvinos. 2022. Univariate and multivariate linear profiles using max-type extended exponentially weighted moving average schemes. *IEEE Access* 10:6126–46. doi:10.1109/ACCESS.2022.3142245.

Noorossana, R., M. Eyvazian, A. Amiri, and M. A. Mahmoud. 2010b. Statistical monitoring of multivariate multiple linear regression profiles in Phase I with calibration application. *Quality and Reliability Engineering International* 26 (3):291–303. doi:10.1002/qre.1066.

Noorossana, R., M. Eyvazian, and A. Vaghefi. 2010a. Phase II monitoring of multivariate simple linear profiles. *Computers & Industrial Engineering* 58 (4):563–70. doi:10.1016/j.cie.2009.12.003.

Rencher, A. C. 2002. *Methods of multivariate analysis*. Wiley: New York.

Sabahno, H., A. Amiri, and P. Castagliola. 2021. A new adaptive control chart for the simultaneous monitoring of the mean and variability of multivariate normal processes. *Computers & Industrial Engineering* 151:106524. doi:10.1016/j.cie.2020.106524.

Sabahno, H., P. Castagliola, and A. Amiri. 2020a. A variable parameters multivariate control chart for simultaneous monitoring of the process mean and variability with measurement errors. *Quality and Reliability Engineering International* 36 (4):1161–96. doi:10.1002/qre.2621.

Sabahno, H., P. Castagliola, and A. Amiri. 2020b. An adaptive variable-parameters scheme for the simultaneous monitoring of the mean and variability of an autocorrelated multivariate normal process. *Journal of Statistical Computation and Simulation* 90 (8):1430–65. doi:10.1080/00949655.2020.1730373.

Soleimani, P., and R. Noorossana. 2014. Monitoring multivariate simple linear profiles in the presence of between profile autocorrelation. *Communications in Statistics – Theory and Methods* 43 (3):530–46. doi:10.1080/03610926.2012.665554.

Soleimani, P., R. Noorossana, and S. T. A. Niaki. 2013. Monitoring autocorrelated multivariate simple linear profiles. *The International Journal of Advanced Manufacturing Technology* 67 (5-8):1857–65. doi:10.1007/s00170-012-4614-1.

Wang, K., A. B. Yeh, and B. Li. 2014. Simultaneous monitoring of process mean vector and covariance matrix via penalized likelihood estimation. *Computational Statistics & Data Analysis* 78 (1):206–17. doi:10.1016/j.csda.2014.04.017.

Yeganeh, A., S. A. Abbasi, and S. C. Shongwe. 2021. A novel simulation-based adaptive MEWMA approach for monitoring linear and logistic profiles. *IEEE Access* 9: 124268–80. doi:10.1109/ACCESS.2021.3107482.

Zhang, J., Z. Li, and Z. Wang. 2009. Control chart based on likelihood ratio for monitoring linear profiles. *Computational Statistics & Data Analysis* 53 (4):1440–8. doi:10.1016/j.csda.2008.12.002.

Zhang, J., Z. Li, and Z. Wang. 2010. A multivariate control chart for simultaneously monitoring process mean and variability. *Computational Statistics & Data Analysis* 54 (10):2244–52. doi:10.1016/j.csda.2010.03.027.

Zou, C., X. Ning, and F. Tsung. 2012. LASSO-based multivariate linear profile monitoring. *Annals of Operations Research* 192 (1):3–19. doi:10.1007/s10479-010-0797-8.